THE UNIVERSITY OF MICHIGAN

COLLEGE OF ENGINEERING
Department of Meteorology and Oceanography

Technical Report

THE CALCULATION OF LONG-WAVE RADIATIVE TRANSFER IN PLANETARY ATMOSPHERES

S. Roland Drayson
Edward S. Epstein, Project Director

ORA Project 07584

supported by:

NATIONAL SCIENCE FOUNDATION
GRANT NO. GP-4385
WASHINGTON, D.C.

administered through:

OFFICE OF RESEARCH ADMINISTRATION ANN ARBOR

November 1967

This report was also a dissertation submitted by the first author in partial fulfillment of the requirements for the degree of Doctor of Philosophy in The University of Michigan, 1967.

ACKNOWLEDGMENT

The author wishes to express his thanks to all those who assisted him in this study. In particular, the guidance and help of Professor Edward S. Epstein, Chairman of the Doctoral Committee, is deeply appreciated. Professor Charles Young gave much assistance and participated in many helpful discussions with the author. The author is also grateful to the other members of the Doctoral Committee, Professors E. Wendell Hewson and Leslie M. Jones, for their interest and willingness to help.

A number of helpful discussions on the form of the equations for the source function were held with Professor William R. Kuhn. Mr. J. W. Peterson kindly provided unpublished falling sphere temperature profiles to use in the cooling rate calculations. The interest and encouragment of other colleagues at the High Altitude Engineering Laboratory is gratefully acknowledged.

The author is grateful for financial support from the National Science Foundation under Grant NO. NSF GP-4385. In addition to this work undertaken in the Department of Meteorology and Oceanography, much of the necessary background material was obtained at the High Altitude Engineering Laboratory, Department of Aerospace Engineering under contracts Nos. Cwb-11376 and Cwb-11106 with the Environmental Science Services Administration and contract No. NASx-54(03) with the National Aeronautics and Space Administration.

TABLE OF CONTENTS

	Page
LIST OF TABLES	v
LIST OF FIGURES	vi
LIST OF SYMBOLS	vii
ABSTRACT	ix
CHAPTER	
1. INTRODUCTION	1
2. THE NUMERICAL EVALUATION OF THE EQUATIONS OF RADIATIVE TRANSFER	4
2.1 Equations of Radiative Transfer	4
2.2 The Evaluation of the Equations of Transfer	8
2.3 Atmospheric Transmissivities	9
2.3.1 Homogeneous Path Absorption	10
2.3.2 Atmospheric Slant Path Absorption	20
2.4 Numerical Procedures for Evaluating Radiative Flux	28
2.4.1 The Isothermal Layer Approximation	28
2.4.2 Polynomial Representation of the Source Function	32
2.5 Conclusions	41
3. APPLICATION TO THE EARTH'S MESOSPHERE AND MESOPAUSE	43
3.1 General Survey of Long-Wave Radiative Transfer in the Earth's Atmosphere	43
3.2 Equations for the Source Functions in the Upper Atmosphere	48
3.3 Calculation Details	57
3.4 Results of Calculations and Comparison with Previous Results	59
3.4.1 Cooling Rates for Model Atmospheres	59
3.4 2 Cooling Rates for Measured Temperatures Profiles	73
3.4.3 Comparison with Previous Calculations	80
3.5 Summary and Conclusion	82
4. APPLICATION TO THE ATMOSPHERE OF MARS	84
4.1 Introduction	84
4.2 Atmospheric Composition	85

TABLE OF CONTENTS (Concluded)

	Page
4.3 Calculation Details and Results	86
4.4 Comparison with Previous Calculations	91
5. CONCLUSIONS	93
6. SUGGESTIONS FOR FUTURE WORK	96
APPENDIX: THE POLYNOMIAL APPROXIMATIONS OF EXPONENTIAL INTEGRALS	98
BIBLIOGRAPHY	105

LIST OF TABLES

Table		Page
I.	Band Intensities Used In Calculating Rotational Line Intensities	60
II.	Relative Abundance Of Isotopic Molecules	60
III.	Cooling Rates In deg K/day For The Individual Bands, U.S. Standard Atmosphere (1962), $\lambda_o = 10^{-5}$ Secs.	62
IV.	Ratio J/B For Individual Bands, U.S. Standard Atmosphere (1962), $\lambda_o = 10^{-5}$ Secs.	63
V.	Heating Rate Coefficients For The Martian Atmosphere	90
VI.	Heating Rates In The Martin Atmosphere For Typical Temperature Profiles.	91
VII.	Coefficients For The Polynomial Approximation Of $E_4(x)$	102
VIII.	Coefficients For The Polynomial Approximation Of $E_3(x)$	103
IX.	Coefficients For The Polynomial Approximations Of $E_2(x)$	104

LIST OF FIGURES

Figure		Page
1.	Diagram of the source function as a function of height.	30
2.	Typical polynomial fits to vertical temperature structures.	35
3.	Calculated cooling rates for the U.S. Standard Atmosphere (1962).	65
4.	Calculated cooling rates for modified U.S. Standard Atmosphere (1962).	68
5.	Calculated cooling rates for ARDC-1959 atmosphere.	71
6.	Calculated cooling rates for CIRA-1961 atmosphere.	72
7.	Calculated cooling rates for measured temperature profiles.	75
8.	Model of the Martian atmosphere.	87

LIST OF SYMBOLS

b	subscript denoting boundary
b_i	line shape factor of ith line
$B(\nu,T)$	Planck black-body function
c	velocity of light in vacuum
E	number density in vibrational quanta
$\bar{E}$	value of E when vibrational energies have a Boltzmann distribution
$E_n(x)$	exponential integral of order n
e_ν	emission coefficient
g	subscript denoting ground
g_i	statistical weight of ith energy level
h	Planck constant
H	flux divergence in quanta cm^{-3} sec^{-1}
$I(\nu,\tau,\mu)$	specific intensity
$J(\nu,\tau)$	source function
k	Boltzmann constant
k_ν	absorption coefficient
M	molecular weight
N	number density of absorbing molecules
p	pressure
S	total band intensity
S_i	intensity of ith line

T	temperature
u	optical mass of absorbing gas
α_D	Doppler half-width
α_L	Lorentz half-width
α_N	natural half-width
$\gamma(\tau,\nu)$	transmissivity
Θ	zenith angle; radiative lifetime
λ	vibrational relaxation time
λ_o	value of λ at 1 atmosphere pressure
μ	cosine of zenith angle
ν	frequency
ν_o	frequency of band center
ϕ	azimuth angle
τ	optical thickness

ABSTRACT

A method is developed for calculating long-wave radiative transfer in a plane parallel atmosphere. Modern computing techniques are used to avoid approximations commonly used in existing methods. Two applications involving the 15μ bands of CO_2 are given, the first to the earth's mesosphere and lower thermosphere, taking vibrational relaxation into account and the second to the Martian atmosphere, for use in a simple atmospheric circulation model.

Although the basic equations of radiative transfer in a plane parallel atmosphere are simple, their solution is a difficult task because of the complicated nature of molecular absorption spectra and because planetary atmospheres are inhomogeneous. In this study atmospheric radiative fluxes and flux divergences are obtained by direct integration with respect to frequency across the absorption bands. The atmosphere is divided into horizontal layers which may be made arbitrarily thin. The direct integration method allows the Curtis-Godson approximation to be applied over successive thin layers, rather than thick atmospheric layers. Band models are not used, but instead the accurate contribution of all lines in the absorption band is calculated at each frequency quadrature point. Rather than using an approximation diffusivity factor, angular integration is performed exactly and expressed in terms of exponential integrals. Accurate, fast computing subroutines, using polynomial approximations, were developed for exponential integrals of the second, third, and fourth orders. Within each horizontal atmospheric layer the source function is assumed to be linear in pressure. This is shown to be more accurate than the assumption of isothermal layers and less problematic than the use of high order polynomials. To avoid numerical difficulties when the atmospheric layers are thin, flux divergences are calculated directly, rather than subtracting fluxes at adjacent levels.

Long-wave radiative transfer in the earth's atmosphere between about 60 and 100 km is dominated by the 15μ CO_2 bands. The radiative transfer equations are solved separately to obtain source functions for each of the bands in this spectral region and hence obtain their contributions to the total cooling rate. Values of vibrational relaxation time in the range 2×10^{-6} to 2×10^{-5} sec at 1 atmosphere are used. Calculations are described for several model atmospheres. In general small amounts of heating are obtained near the mesopause corresponding to discontinuities in temperature gradients which characterize most models. Vibrational relaxation affects the cooling rate above about 75 km, although the less abundant isotopic molecules depart from L.T.E. near 60 km. Measured, as opposed to mean, temperature soundings also are used to calculate cooling rates. These show that the local temperature structure largely determines the radiative transfer and produces a predominance of cooling, rather than heating near the mesopause. The mean cooling is significantly greater than the cooling calculated from the mean profiles, suggest-

ing the presence of a mean heat sink for this part of the atmosphere, important for energy balance considerations.

In the Martian atmosphere, the 15μ CO_2 bands must also dominate the long-wave radiative transfer. Flux divergences are calculated for a simple model atmosphere, assuming pure CO_2 and a surface pressure of 6 mb. Since the results are for use in a general circulation model, the cooling rates are expressed as a simple function of the temperature profile, so that rapid computations can be made. The cooling rates for several temperature profiles are presented.

CHAPTER 1

INTRODUCTION

Although the atmosphere, oceans and land masses of the earth constitute an extremely complicated system for the transfer of energy, the long time-scales of terrestrial climatic changes imply that for the system viewed as a whole there must be a close balance between the solar energy absorbed and the long-wave radiant energy lost to space. The radiative and dynamic processes are not separate, but are related in a complex manner. For example, the presence of clouds affects the amount and distribution of solar energy received and modifies the out-going long-wave radiation. Some of the main features of the vertical atmospheric temperature profile can be accounted for by radiative processes, but dynamic processes e.g., convection must be introduced to account for other features.

Similar processes occur in the atmospheres of other planets. In the Martian atmosphere, radiative processes are simpler; the absence of oceans on the surface, the virtual absence of water vapor and ozone in the atmosphere and the rarity of clouds provide a much less complicated environment than that of the earth. On the other hand, Venus is permanently shrouded in clouds of an unknown composition, making the atmosphere the object of considerable speculation, and the problem of radiative transfer unsolvable at present.

In recent years, the development of meteorological satellites has renewed interest in atmospheric radiative processes. By making suitable

measurements of the outgoing radiation field, it is possible to infer information on the vertical temperature structure of the atmosphere and on the distribution of water vapor and ozone. A polar orbiting satellite can provide global coverage at regular intervals. In order to extract the maximum amount of information from the measurements, a detailed accurate knowledge of atmospheric radiative processes is required, so that developments in this field have led to important theoretical advances.

Possible modification of the radiative regime by air pollution is of considerable interest and importance, particularly that due to the steady increase in the amount of carbon dioxide in the atmosphere formed by the combustion of fossil fuels. The long-term effect of this increase is difficult to gauge because of the complicated interaction of radiative and dynamic processes, but if the net result is to increase the surface temperature of the earth by as little as 1°C it might be sufficient to melt large amounts of polar ice and cause flooding over low-lying regions of the earth where much of the population is concentrated.

The development of electronic computers has made possible the theoretical study of the general circulation of the atmosphere by means of numerical models and the development of numerical weather prediction. In these models radiative transfer is approximated in only a rather crude manner. Refinements in this area are essential, particularly for long-range forecasting. When the role which radiative transfer plays in the general circulation is understood, problems such as the influence of the

carbon dioxide concentration in the atmosphere will be solvable.

The mathematical equations governing atmospheric long-wave radiative transfer are comparatively simple. However the structure of atmospheric absorption bands is exceedingly complicated and some aspects such as the shapes of spectral absorption lines are not yet fully understood. The variations of temperature, pressure and absorber concentration in the atmosphere combine to make the solution of the transfer equation a task of extreme difficulty. Many approximations were introduced before electronic digital computers were available.

It is now practicable to solve the equations more precisely. The purpose of this study is to develop a numerical method of solution of the radiative transfer equations with as few approximations as possible, using modern computing techniques. Direct integration with respect to frequency has already been applied to the calculation of atmospheric slant path transmissivities. In this study the technique is extended to the calculation of radiative fluxes and flux divergences and is shown to be flexible and accurate.

A critical discussion of many existing approximations is contained in Chapter 2, where the method of solution of the equations of radiative transfer is developed. The results are applied to two atmospheric radiative problems. Chapter 3 is devoted to an analysis of the role of the 15 μ bands of carbon dioxide in the earth's upper atmosphere, including the deviation from local thermodynamic equilibrium. Chapter 4 concludes the study with a radiative transfer calculation for application to a Martian atmospheric circulation model.

CHAPTER 2

THE NUMERICAL EVALUATION OF THE EQUATIONS OF RADIATIVE TRANSFER

2.1 EQUATIONS OF RADIATIVE TRANSFER

In deriving the equations of radiative transfer the following assumptions will be made.

(a) The atmosphere is plane-parallel and horizontally homogeneous.

(b) Atmospheric refraction can be neglected.

(c) Scattering effects at the wavelengths under consideration may be neglected.

(d) The source function $J(\nu,\tau)$ is isotropic.

The differential equation may be written, as in Chandrasekhar 1960, p. 9,

$$\mu \frac{dI(\nu,\tau,\mu)}{d\tau} = I(\nu,\tau,\mu)-J(\nu,\tau) \qquad (2.1.1)$$

where $I(\nu,\tau,\mu)$ is the specific intensity at frequency ν and zenith angle Θ

μ = $\cos\Theta$

τ_ν is the optical thickness, defined by $d\tau = k_\nu du$

u is the optical mass of the absorbing gas

k_ν is the absorption coefficient

e_ν is the emission coefficient

$J(\nu,\tau)$, the source function, is the ratio e_ν/k_ν

For a gas in local thermodynamic equilibrium, the source function is equal to the Planck black-body function. The form of the source function

for radiating gas which is not in local thermodynamic equilibrium will be discussed in a later section.

The usual convention will be followed here, that τ_ν is zero at the top of the atmosphere and increases with increasing pressure.

A formal solution of Eq. (2.1.1) may be found in any text on radiative transfer e.g., Goody (1964).

$$I(\nu,\tau,\mu) = I(\nu,\tau_b,\mu)e^{-(\tau_b-\tau)/\mu} + \int_\tau^{\tau_b} J(\nu,t)e^{-(t-\tau)/\mu}\frac{dt}{\mu} \quad (2.1.2)$$

where τ_b is the value of τ at the boundary. For values of $\mu > 0$ this boundary is the lower boundary of the atmosphere (the planetary surface). It is convenient to assume that $I(\nu,\tau_b,\mu)$ is independent of μ, although this assumption is not strictly correct. Its applicability depends on the angular distribution of specific intensity incident upon the surface, as well as its diffuse reflectance properties, which may be complicated functions of the incidence and reflection angles, and may vary also with frequency. Adequate experimental studies have not been made, either for the case where the lower boundary surface is a cloud layer, or where it is the ground, consisting of soil, bare rock and vegetation. Except within the planetary boundary layer, this assumption is probably not important. It will also be convenient to assume that $I(\nu,\tau_b)$ is given by the black body source function $B(\nu,T_g)$ at frequency ν and the temperature T_g of the surface. Frequently T_g will be taken equal to the temperature of the atmosphere bounding the surface.

For $\mu < 0$ the boundary is the top of the atmosphere, and any radiation incident upon it will be neglected, i.e.,

$$I(\nu,0,\mu) = 0 \quad \text{for } \mu < 0$$

With these assumptions Eq. (2.1.2) may be rewritten

$$I(\nu,\tau,\mu) = B(\nu,T_g)e^{-(\tau_g-\tau)/\mu} + \int_\tau^{\tau_g} J(\nu,t)e^{-(t-\tau)/\mu}\frac{dt}{\mu} \quad (\mu > 0) \tag{2.1.3a}$$

$$I(\nu,\tau,\mu) = \int_0^{\tau} J(\nu,t)e^{-(t-\tau)/\mu}\frac{dt}{\mu} \quad (\mu < 0) \tag{2.1.3b}$$

The flux across any horizontal surface at pressure p is defined by

$$F(p) = \int_\nu \int_{\mu=-1}^{+1} \int_{\phi=0}^{2\pi} I(\nu,\tau,\mu)\ \mu\ d\phi\ d\mu\ d\nu$$

Now the specific intensity I_ν is independent of the azimuth angle ϕ, so that the equation may immediately be reduced to a double integral

$$F(p) = 2\pi \int_\nu \int_{\mu=-1}^{+1} I(\nu,\tau,\mu)\ \mu\ d\mu\ d\nu \tag{2.1.4}$$

To obtain the rate of loss of energy at any point, the flux divergence must be evaluated

$$\frac{dF}{dp} = 2\pi \int_\nu \int_{-1}^{+1} \mu \frac{dI}{dp}\, d\mu\, d\nu \tag{2.1.5}$$

Substitution of Eq. (2.1.1) enables the flux divergence to be written in the form

$$\frac{dF}{dp} = 2\pi \frac{du}{dp} \int_\nu \int_{-1}^{+1} [I(\nu,\tau,\mu)-J(\nu,\tau)]k_\nu\, d\mu\, d\nu \tag{2.1.6}$$

If the source function $J(\nu,\tau)$ is known at every level in the atmosphere, the flux divergence can be found, in theory at least, by substituting the values of $I(\nu,\tau,\mu)$ evaluated from Eqs. (2.1.3a) and (2.1.3b) into Eq. (2.1.6) and integrating over μ and ν. In practice this procedure is very complicated, since k_ν is a rapidly varying function of frequency, and is also pressure and temperature sensitive. Much effort has been devoted to the investigation of approximations which enable Eq. (2.1.6) to be evaluated while maintaining a high degree of accuracy.

Equation (2.1.6) gives the flux divergence at a single level in the atmosphere. In atmospheric energy balance studies it is frequently important to know the rate of loss of energy averaged over a layer, rather than the flux divergence at a point. The average value may be found by evaluating Eq. (2.1.4) at the boundaries of the layer, and subtracting the fluxes. This finite difference method is made difficult by the fact that at low pressures small differences in flux at adjacent levels can result in large cooling rates; it is essential to ensure that the noise introduced by the numerical processes used in the calculations does not mask the true flux difference.

In spite of these difficulties the last method is the one employed in this study, with suitable precautions to ensure the suppression of such noise. However, Eq. (2.1.6) provides a valuable physical insight into the radiative transfer process and will be referred to frequently.

2.2 THE EVALUATION OF THE EQUATIONS OF TRANSFER

To evaluate the flux F(p) at the pressure level p, the values of I_ν are subsituted from Eqs. (2.1.3a) and (2.1.3b)

$$F(p) = 2\pi \int_\nu \{\int_0^1 [B(\nu,T_g)\mu e^{-(\tau_g-\tau)/\mu} + \int_\tau^{\tau_g} J(\nu,t)\mu\, e^{-(t-\tau)/\mu}\, \frac{dt}{\mu}]d\mu$$

$$+ \int_{-1}^{0} [\int_0^\tau J(\nu,t)\mu\, e^{-(t-\tau)/\mu}\, \frac{dt}{\mu}]d\mu\}\, d\nu \qquad (2.2.1)$$

At this point the formulation can be simplified by the introduction of the exponential integral $E_n(x)$ defined by

$$E_n(x) = \int_0^1 e^{-x/\mu}\, \mu^{n-1}\, \frac{d\mu}{\mu} \quad n = 0,1,2\ldots, \quad x \geq 0 \qquad (2.2.2)$$

The exponential integrals have a number of useful properties which are readily proved. In particular the following will be employed

$$\frac{dE_n(x)}{dx} = -E_{n-1}(x) \quad n = 1,2\ldots, \; x \geq 0 \qquad (2.2.3a)$$

$$E_{n+1}(x) = \frac{1}{n}\,[e^{-x}-xE_n(x)] \quad n = 0,1,\ldots, \; x \geq 0 \qquad (2.2.3b)$$

F(p) can then be expressed as

$$F(p) = 2\pi\int_\nu \{B(\nu,T_g)E_3(\tau_g-\tau)-\int_0^\tau J(\nu,t)E_2(\tau-t)dt+\int_\tau^{\tau_g} J(\nu,t)E_2(t-\tau)dt\}d\nu$$

The integral with respect to t may be transformed by integration by parts using relation (2.2.3a), yielding

$$F(p) = 2\pi\int_\nu \{ [B(\nu,T_g)-J(\nu,\tau_g)]E_3(\tau_g-\tau) + E_3(\tau)J(\nu,0) + \int_o^{\tau_g} \frac{dJ}{dt} E_3(|t-\tau|)dt\}d\nu \quad (2.2.4)$$

The expression for the flux divergence may be treated in a similar way. Substituting Eqs. (2.1.3a) and (2.1.3b) into Eq. (2.1.6), and integrating by parts

$$\frac{dF}{dp} = 2\pi \frac{d\mu}{dp} \int_\nu k_\nu \{\int_\tau^{\tau_g} E_2(t-\tau)\frac{dJ}{dt}dt-\int_o^{\tau} E_2(\tau-t)\frac{dJ}{dt}dt-E_2(\tau)J(\nu,0)\}d\nu \quad (2.2.5)$$

The last two equations involve three integrations, over frequency, over height, and over zenith angle (the latter being expressed as the exponential integral). Each of the integrations presents some difficulty. Before discussing techniques for performing the integrations, it is of interest to examine the problem of calculating atmospheric transmissivities, and the form of the absorption coefficient k_ν.

2.3 ATMOSPHERIC TRANSMISSIVITIES

The calculation of transmissivities along an atmospheric slant path is a complicated problem. Part of the complexity arises because the temperature, pressure and concentration of the absorbing gas may vary along the path. Even in the absence of such variations, i.e., for homogeneous absorption paths, the difficulties are sufficiently great to have merited a large number of both experimental and theoretical investigations during the last twenty years. However, the comparative simplicity of the homogenous path absorption has led to non-homogeneous path absorption being ex-

pressed in an approximate way in terms of an 'equivalent' homogeneous path. Furthermore, homogeneous path theoretical calculations can easily be compared with experimental laboratory absorption measurements. Thus, it is of considerable interest to examine the simpler case in detail.

2.3.1 Homogeneous Path Absorption

The results of experimental determinations of absorption are used in all methods of calculating transmissivities. The experimental values may be used directly if measurements have been made over a wide range of pressure, optical mass and temperature, and interpolated for the actual conditions required. However, the method has some serious limitations. Accurate absorption measurements are difficult to make at low pressure and for short paths where the transmissivity is near unity. Few data are available at temperatures below those normally encountered in the laboratory, such as are found in the earth's mesosphere, for example. In addition, very long paths, important for spectral regions where the absorption is weak, are impossible to simulate in the laboratory, frequently leading to extrapolation, rather than interpolation.

A typical infrared absorption band consists of a large number of individual absorption lines, many of which may be resolved experimentally under suitable physical conditions. The frequency at the centers of these lines may be measured quite accurately, or calculated theoretically once the values of the relevant parameters have been experimentally determined (Hertzberg 1945). If the intensity of each line can be accurately measured,

and the line shape and half-width are adequately known, it is possible to calculate the transmissivity γ_ν at any frequency ν by the relation

$$\gamma_\nu = \exp(-\tau_\nu) \tag{2.3.1}$$

In general, τ_ν will be equal to the sum of optical thicknesses of the different absorbing gases. Where there is only one absorbing gas

$$\tau_\nu = k_\nu u \tag{2.3.2}$$

where k_ν is the absorption coefficient and u the optical mass of the absorption path. k_ν is the sum of the absorption coefficients of all the spectral lines:

$$k_\nu = \sum_{i=1}^{N} {}_ik_\nu \tag{2.3.3}$$

The absorption coefficient of the ith line, center ν_i is given by

$${}_ik_\nu = S_i\, b_i(\nu_i,\nu) \tag{2.3.4}$$

where S_i is the intensity of the ith line, and b_i is a line shape factor for the ith line, normalized so that

$$\int_0^\infty b_i(\nu_i,\nu)\, d\nu = 1 \tag{2.3.5}$$

There are two classical line shapes which may be regarded as limiting cases in the spectral region and under the physical conditions that are considered here.

(a) Lorentz line shape, valid when the line broadening is due to

molecular collisions of the excited molecules, thus perturbing the energy level. In this case

$$b_i(\nu_o,\nu) = \frac{1}{\pi} \frac{\alpha_i}{(\nu-\nu_o)^2+\alpha_i^2} \qquad (2.3.6)$$

α_i is the Lorentz half-width (i.e., the half-width at half maximum).

(b) Doppler line shape, caused by the Doppler shift due to the thermal motion of the molecules.

$$b_i(\nu_o,\nu) = k_o \exp(-x^2) \qquad (2.3.7)$$

where

$$k_o = \frac{1}{\alpha_D} \left(\frac{\ell n 2}{\pi}\right)^{1/2}$$

$$x = \frac{\nu-\nu_o}{\alpha_D} (\ell n\ 2)^{1/2}$$

and α_D is the Doppler half-width

Natural broadening has a half-width α_N defined by

$$\alpha_N = \frac{\pi c}{\theta}$$

where

c is the velocity of light in vacuum

and

θ is the radiative life-time of the excited state

In all cases the natural half-width is much smaller than the Doppler half-

width and, except at extremely low pressures, much less than the Lorentz half-width and can be neglected.

The Lorentz half-width α_L is dependent on temperature and pressure; for most gases the relation may be expressed by

$$\alpha_L = \alpha_o \frac{p}{p_o} \sqrt{\frac{T_o}{T}} \tag{2.3.8}$$

where α_L is the half-width at temperature T and pressure p and α_o is the half-width at temperature T_o and pressure p_o. It should be noted that α_o does not normally have the same value for all lines in an absorption band. On the other hand, α_D is given by

$$\alpha_D = \frac{\nu_o}{c} \left(\frac{2kT\ell n2}{M} \right)^{1/2}$$

where k is the Boltzmann constant and M is the molecular weight. Thus α_D varies only slowly from line to line across an absorption band.

Over a wide range of atmospheric pressures it is found that both the Doppler and Lorentz broadening are important. The correct line shape for the mixed Doppler-Lorentz broadening is given by a convolution of the line shapes.

$$b(\nu_o,\nu) = \frac{k_o y}{\pi} \int_{-\infty}^{\infty} \frac{e^{-t^2}}{y^2+(x-t)^2} \, dt \tag{2.3.9}$$

where

$$y = \frac{\alpha_L}{\alpha_D} (\ell n2)^{1/2}$$

The resulting integral cannot be evaluated analytically, but a number of numerical methods have been developed. The method adopted here is that of Young (1965), with two modifications (Drayson and Young, 1966).

(i) The range of Hermite-Gauss quadrature was extended to the region

$$y \geq 0, \quad x \geq 7.0$$

(ii) 4-point Hermite-Gauss quadrature was used over this entire region.

Although the Lorentz line shape gives a good approximation when the broadening process is due to molecular collisions, important deviations have been observed for a number of molecules. For instance, Winters et al., (1964) have shown that beyond about 5 cm^{-1} from the line center the absorption coefficients for lines in the 4.3 μ CO_2 band are less than those predicted by the Lorentz line shape. The deviations are dependent on the broadening gas, being less pronounced for nitrogen broadened CO_2 than for pure CO_2. Burch et al., (1965) have verified these results and made similar measurements in other CO_2 absorption bands, where qualitatively the same phenomena were observed, but with different magnitude of deviation. These absorption measurements have been made in regions free from strong lines, where the absorption is due to the wings of strong lines situated a few wavenumbers away. The absorption coefficient under these conditions changes only slowly with frequency, so that the instrumental response function does not appreciably distort the absorption curve.

It is more difficult to examine the shape near the line center, since

the best spectrometers have a resolution in the infrared comparable to the Lorentz half-width at about 1 atmosphere. Raising the pressure much higher than this causes the lines to overlap appreciably in most absorption spectra. However, it is not unreasonable to expect deviations closer to the line center. Indeed, Burch et al., (1965) have indirectly shown this to be true for CO_2 by comparing the absorption of the self-broadened and nitrogen-broadened gas. Burch et al., found that the line shapes of the two samples were different, implying that one at least is non-Lorentzian. Investigations using a laser as an essentially monochromatic source may be able to yield information on line half-width and shape.

In a recent report, Ray et al., (1966) have advanced the idea that the non-Lorentzian effects may, in part at least, be due to the geometry of the absorption cell, an effect that would not be present in a real atmospheric slant path.

In this study the Lorentz line shape is assumed to be completely valid. At the present time the deviations are neither sufficiently understood on theoretical grounds, nor adequately measured experimentally, particularly at low concentrations such as the carbon dioxide mixing ratio in the earth's atmosphere, to warrant modification of the line shape. This is not a limitation of the methods developed and described here, since any line shape can easily be incorporated into the calculations. In most cases the effect of deviations from the Lorentz line shape on the radiative cooling rates is probably small.

It will now be assumed that the line shapes and half-widths are adequately known, and that the line intensities have also been precisely determined. Using Eq. (2.3.1), it is possible to calculate the transmissivity γ_ν at any desired frequency ν. In practice, however, it is usually desirable to calculate the average value of γ_ν over some finite frequency interval $\Delta\nu$.

$$\overline{\gamma} = \frac{1}{\Delta\nu} \int_{\Delta\nu} \gamma_\nu \, d\nu \qquad (2.3.10)$$

The interval $\Delta\nu$ may contain a large number of absorption lines, and there may be many more lines outside the interval which contribute to the absorption within the interval. Thus γ_ν may be a rapidly fluctuating function of ν whose value is a complicated function dependent on the position, intensity and line shape of many individual absorption lines. To overcome some of these difficulties the concept of the band model was introduced. Band models approximate the actual distribution of line positions and intensities in such a way that a solution of integral (2.3.10) may be more easily obtained, the solution often being expressed in terms of analytic of semi-analytic functions.

The simplest case, a single isolated line with the Lorentz shape, was solved by Ladenberg and Reiche (1913). The result can be extended to any number of lines, provided that they do not overlap. The Regular or Elsasser band (Elsasser, 1938) applies to an infinite array of Lorentzian lines of equal half-width and intensity, equally spaced. It simulates quite well the conditions encountered in the P and R branches of certain

bands e.g., the fundamental in the 15 μ CO_2 bands. This model has been generalized to include a random superposition of different Elsasser bands in the Random Elsasser model.

The Elsasser band and its derivatives are useful for some molecular absorption bands, but for others such as water vapor and ozone there is little suggestion of regularity. The lack of regularity prompted the development of the Statistical or Random model, suggested independently by Goody (1952) and Mayer (1947). The distribution and intensity of the lines is defined by probability functions which may be varied to suit the actual distributions.

In addition to these important band models, numerous other models are scattered throughout the radiative transfer literature, most being modifications or refinements of those described above. Band models have played an extremely important role in understanding radiative transfer processes in the atmosphere, transforming what would otherwise have been a problem of impossible complexity into one of manageable proportions. But it is important to realize that band models do have limitations and that alternative procedures are now available. The limitations include the following:

(i) The spectral resolution of the transmittances is finite: for the Elsasser model it is a multiple of the line spacings, while the statistical model must use an averaging interval sufficiently large to ensure that the true distribution of the lines is adequately simulated by the statistical distribution. The finite resolution introduces further compli-

cations for atmospheric slant paths.

(ii) Many band models do not allow for accurate contributions of the wings of lines lying outside the spectral region under consideration.

(iii) The actual distribution of lines can only be approximated by the band models. In some regions, e.g., near Q-branches, it is extremely difficult, if not impossible, to accurately account for the complex distribution of lines. The development of the Quasi-Statistical or Quasi-Random model by Kaplan (1953) and Wyatt et al., (1962) has done much to overcome these objections. The resolution of the transmittances can be made arbitrarily small, the wings are accurately allowed for and the actual distribution of lines can be approached for sufficiently small averaging interval. It shares one problem with the other models:

(iv) When the models permit accurate calculation of the absorption due to a real absorption band, the complexity and length of calculation is considerable, even for the Lorentz line shape. For other line shapes including the mixed Doppler-Lorentz line shape, the complexities are even greater.

Extensive tables using the Quasi-Random model have been prepared (Stull et al., 1963). In an effort to reduce computing time an averaging interval of $\delta = 5$ cm^{-1} was used; this violates a basic requirement of the model, that δ should be sufficiently small to allow the lines within each δ-interval to be assumed randomly distributed. In the 15 μ CO_2 bands this violation resulted in the Q-branches being considerably enhanced, overestimating the total absorption appreciably (Drayson 1964).

Modern computing techniques have made possible an alternative simpler approach, using direct numerical integration of Eq. (2.3.1). At each frequency quadrature point the contribution from all lines is evaluated accurately. The numerical accuracy of the calculations can be increased by making the quadrature intervals sufficiently small, especially in the neighborhood of line centers. Five significant figures are easily achieved. Computation time can be reduced by careful programing and the use of interpolative procedures for more distant lines (Drayson & Young 1966).

This method of direct integration was first employed over a limited range in the 9.6 μ ozone bands by Hitchfeld and Houghton, (1961) and has since been employed by a number of authors in studies of several molecular absorption bands. The advantages of these methods are:

(i) The resolution is not limited; the transmissivities may be weighted by an instrumental response function and compared with high resolution experimental spectra.

(ii) There is considerably more flexibility in the calculations, especially when extended to non-homogeneous paths as in Section (2.3.2).

(iii) The actual distribution of line positions and intensities is used and all contributions from the wings of distant lines are accurately included.

Comparisons between theoretical calculations using direct integration techniques and experimental laboratory data do not always show good agreement. Indeed, the application of these techniques has shown that previously accepted values of band parameters are considerably in error. Part of the

discrepancy is due to experimental error, but this is probably much smaller than the error introduced in attempting to deduce the parameters from the measurements. Measurements on the same band by different experimenters produce widely differing estimates, often with mutually inconsistent error estimates, as in for example, Drayson and Young (1966). There is a clear need for accurate, well-designed experiments, coupled with a careful analysis to yield the desired band parameters.

2.3.2 Atmospheric Slant Path Absorption

Calculations of absorption over atmospheric slant paths are more complicated than the case discussed above, because of variations in the pressure, temperature and absorber concentration. Eq. (2.3.2) must now be generalized to the form:

$$\tau_\nu = \int_u k_\nu \, du \qquad (2.3.11)$$

the integral being taken along the absorption path. Variations in the three parameters affect the integral in the following ways:

(a) The Lorentz half-width varies directly with pressure and inversely with the square root of temperature. It is also a function of absorber concentration.

(b) The Doppler half-width varies directly with the square root of temperature.

(c) The line intensities are complicated functions of temperature. Typically the intensities of very strong lines decrease slowly with increasing

temperature. Lines belonging to weak bands increase in intensity very rapidly with increasing temperature, as much as an order of magnitude for a 25°K temperature rise, which has prompted the use of the term 'hot band' to describe them.

Generally, the practical problem of calculating slant path absorption has been restricted to average values of the transmissivity $\overline{\gamma}$, defined in Eq. (2.3.10). Of the several methods suggested, the one of most practical importance is the Curtis-Godson approximation (Curtis, 1952 and Godson 1953). This method seeks to find a mean pressure $\overline{p}$, temperature $\overline{T}$ and a optical mass $\overline{u}$ such that the transmission is approximated by a homogeneous absorption path with these three physical parameters. The expressions for $\overline{p}$, $\overline{T}$ and $\overline{u}$ are required to satisfy the criterion that the limiting cases of weak line and strong line absorption shall be accurately represented.

The expressions for $\overline{u}$ and $\overline{p}$ are simplest when the temperature is constant along the absorption path, and has been most thoroughly investigated to test its accuracy. Under these conditions

$$\overline{p} = \frac{\int_u p \, du}{\int_u du} \qquad (2.3.12a)$$

$$\overline{u} = \int_u du \qquad (2.3.12b)$$

The errors in the approximation have been investigated for a single isolated line for the case of a uniformly mixed gas such as carbon dioxide in the earth's atmosphere, by Kaplan (1959) and extended to more general

pressure limits by Drayson (1966). The approximation was found to be quite accurate for most applications, although errors of up to about 6% can arise for certain combinations of pressure and line intensity. Similarly, Mayot and Vigroux (1965) found that the Curtis-Godson approximation was not a serious source of error in interpreting observations in the 9.6 μ ozone bands.

In radiative transfer calculations the computation of transmissivities is only an incidental procedure, and an approximation should be regarded as valid only if it produces accurate values of flux divergence. This much more difficult task was attacked by Walshaw and Rodgers (1963), who calculated the effect of the Curtis-Godson approximation on the accuracy of radiative heating-rate calculations. They considered radiative transfer in the earth's atmosphere in the 9.6 μ ozone bands, the 15 μ carbon dioxide bands and the rotational water vapor band. The Lorentz line shape only was used. Their conclusions were:

(a) For the 15 μ CO_2 bands the approximation is extremely accurate.

(b) In the rotational water vapor bands, the result for the band as a whole is acceptable, although the errors are sometimes larger over small portions of the band.

(c) The approximation is not valid in the 9.6 μ O_3 bands. The failure was attributed to the fact that the ozone mixing ratio in the earth's atmosphere increases with decreasing pressures, a condition for which Curtis (1952) found the approximation to be less accurate.

To simplify their calculations Walshaw and Rodgers did not consider the complicated effect of variations of temperature on the transmissivity. It is interesting to examine the influence of such variations in the earth's atmosphere on a CO_2 line whose intensity increases rapidly with increasing temperature. At the stratopause, where the temperature is a maximum, it will be quite strong compared to the tropopause or mesopuase regions. Carbon dioxide is fairly uniformly mixed up to at least 70 km, but since the transmissivity is a function of the product of the optical mass and the line intensities, it can be seen that the same effect on the transmissivity could be obtained by assuming that the line intensity remained constant and that the CO_2 concentration increases rapidly at the stratopause, i.e., a situation similar to that of ozone where the higher concentration is at the lower pressure, a circumstance which may lead to considerable error in the Curtis-Godson approximation. Moreover, because of the large number of moderately weak temperature-sensitive lines, they exert considerable cooling influence at the stratopause level and must be accurately calculated.

The Curtis-Godson approximation is designed to give an estimate of the average transmission over a finite frequency interval. At pressures where the Lorentz line shape is valid for homogeneous absorption paths, the Curtis-Godson approximation still gives a Lorentz line shape for the slant path, whereas the true line shape has more absorption at the line center and less in the wings, tending to a common value in the far wings (Goody, 1964).

The methods developed in this paper are designed to be applied to all gases of atmospheric interest, regardless of their distribution and temperature dependence of line intensity. Fortunately, the direct integration technique provides the flexibility to avoid some of the difficulties of the Curtis-Godson approximation, which are not easy to apply to band models or empirical data. The solution lies in dividing the atmosphere into horizontal layers over which variations in absorber concentrations and in temperature are small. Two alternatives are then possible:

(a) The Curtis-Godson approximation may then be applied over each of these layers to obtain values of $\overline{p}$, $\overline{u}$, $\overline{T}$. This method was used by Gates et al., (1963), and Drayson and Young (1966).

(b) By assuming a value of $\overline{T}$ in each layer the absorption coefficient may be integrated with respect to pressure, giving a slightly more accurate solution than method a. For carbon dioxide, whose mixing ratio is assumed constant, the solution has been given by Drayson (1966). However, this variation is somewhat cumbersome and offers little advantage over the first method.

To obtain the optical thickness for a path between two arbitrary points in the atmosphere, the sum of the optical thicknesses of the intervening layers is taken. It can easily be seen that this method is equivalent or nearly equivalent in case (b) to approximating the slant path by a series of homogeneous paths; the limiting case where the number of homogeneous paths is reduced to one is the Curtis-Godson approximation in its original form. The method of direct integration with respect to frequency

has previously been applied to the calculation of fluxes and flux divergences e.g., Hitchfeld and Houghton (1961), but the full potential of the method has not been exploited. In previous studies integration with respect to frequency was used to compute average transmissivities. Here it is used to obtain fluxes and flux divergences directly.

The expressions for flux (Eq. (2.2.4)) and flux divergence (Eq. (2.2.5)) do not explicitly contain the transmission function, but rather the exponential integral of the optical thickness. It will be recalled that the exponential integrals were obtained by integration of the transmission function with respect to angle and for this reason the exponential integral is frequently called the diffuse transmission function.

One way to evaluate the integral is to use numerical quadrature. In this case the exponential integral $E_n(\tau)$ is approximated by an expression of the form

$$E_n(\tau) \sim \sum_{i=1}^{N} a_i e^{-b_i \tau} \qquad (2.3.13)$$

$$= \sum_{i=1}^{N} a_i \gamma(b_i \tau)$$

where a_i and b_i $(i = 1,\ldots,N)$ are constants. The advantage of this form is that the diffuse transmission function is expressed in terms of normal transmission functions, and since the source function J is usually a slowly varying function of frequency, and can be considered as effectively constant over a small frequency interval $\Delta\nu$, the expressions for F(p) and dF/dp may be readily integrated with respect to frequency and involve only

the average transmissivity $\overline{\gamma}$ over the frequency interval $\Delta\nu$.

The most widely employed approximation for $E_3(\tau)$ is

$$E_3(\tau) \sim \frac{1}{2} \exp(-k\tau) \qquad (2.3.14)$$

which is a special case of Eq. (2.3.13) with N = 1. The use of this form is discussed by Goody (1964). Strictly speaking k is not a constant, but varies as τ varies from 0 to ∞. To maintain accuracy for small values of τ, k should be equal to 2.0, but this value is not a good approximation for larger values of τ. Usually the diffusivity factor k is taken to be 1.66, a value Elsasser (1942) obtained for the strong line approximation of an Elsasser band.

Suppose that an approximation of this form is used in Eq. (2.2.4) to evaluate the flux. The flux divergence is obtained by differentiating Eq. (2.2.5). From Eqs. (2.3.14) and (2.2.3a) we have

$$\begin{aligned} E_2(\tau) &= -\frac{d}{dt} E_3(\tau) \\ &\sim k/2 \exp(-k\tau) \end{aligned}$$

As stated above, k = 2 must be used when $\tau = 0$ and this also gives a poor approximation for $E_2(\tau)$. In a later section an expression for F(p) which involves $E_4(\tau)$ will be derived. This leads to an expression

$$E_4(\tau) \sim \frac{1}{2k} \exp(-k\tau)$$

Since $E_4(0) = 1/3$, it is impossible simultaneously to obtain a good approximation for $E_2(\tau)$, $E_3(\tau)$, $E_4(\tau)$, even at x = 0.

Despite these inaccuracies, the diffusivity factor of 1.66 has been almost universally applied. It is claimed that the errors in flux divergence are small, although it has not really been thoroughly tested under adverse conditions. Probably errors from one part of the absorption band are compensated by cancellation from other parts of the band, reducing the inaccuracies to acceptable levels.

In most physical problems an approximation as crude as Eq. (2.3.14) is not used. There are however two reasons for its use.

(a) The exponential integral is not as easy to evaluate as the exponential function. This was particularly true before the development of electronic computers.

(b) The more important reason is that evaluation of the exponential integral precludes the use of band models. The diffusivity factor approximation used in conjunction with the Curtis-Godson approximation reduces the complex problem of diffuse slant path transmission to a much simpler 'equivalent' homogeneous path over a finite frequency interval, where empirical data or band model calculations may be used.

In the calculations made in this study, direct integration with respect to frequency is employed, so that the reasoning in b does not apply. A number of methods of evaluating the exponential integrals were examined, but none was found suitable for use in the computer programs of flux divergence because of their slowness or inaccuracy. A series of subroutines using polynomial approximations was developed and is fully described in the appendix. The average execution time of these subroutines was less

than that of the computing system exponential function subroutine. The development of fast subroutines is critical since a large proportion of the execution time of the programs is spent in these subroutines.

2.4 NUMERICAL PROCEDURES FOR EVALUATING RADIATIVE FLUX

For the purposes of this section it will be assumed that the problem of calculating the diffuse transmission function has been overcome and that the source function $J(\nu,p)$ is known at every point in the atmosphere. The flux $F(p)$ given by Eq. (2.2.4) can be evaluated numerically in a straightforward manner, using standard quadrature techniques. However, because of the approximate nature of quadrature evaluations, the calculated flux differs from the true flux by some small error $\epsilon(p)$. The flux difference between two adjacent pressure levels may be found provided it is not of order $\epsilon(p)$. The quantity $\epsilon(p)$ can be reduced by careful quadrature procedures, but will always be present because of round-off and other inaccuracies introduced in computation, i.e., the well-known difficulties of numerical differentiation are encountered.

2.4.1 The Isothermal Layer Approximation

A frequently used method of reducing the numerical noise is to assume that the atmosphere is divided into isothermal layers or, more precisely, layers in which the source function is constant. Equation (2.2.4) is no long valid, since its derivation depends on the continuity of the source function as a function of pressure. Instead Eq. (2.2.1) may be integrated to give

$$F_i = 2\pi\int_\nu \{B(\nu,\tau_g)E_3(\tau_N-\tau_i) - \sum_{j=1}^{N} J_j[E_3|\tau_i-\tau_j| - E_3|\tau_{i\,j-1}-\tau|]\}\, d\nu$$

$$i = 0,1,\ldots N \qquad (2.4.1)$$

where the atmosphere has been divided into N layers and the subscript j refers to the value of the variables at the level j.

The isothermal assumption is, of course, a gross distortion of the temperature profile expected in a planetary atmosphere and since radiative transfer processes tend to smooth temperature profiles, such discontinuities in the temperature field could not exist. The use of the isothermal assumption can be justified only if it gives realistic values of the average flux divergence in a layer.

Consider, as an example, a part of an absorption band where the optical thickness is very large, i.e., the atmosphere becomes opaque within a very short distance. In this case the net flux is small and hence the true flux divergence is small also and independent of the temperature profile. This holds even if the temperature profile is similar to that in Fig. 1. If the isothermal slab approximation is used, the flux can easily be evaluated The assumption that the optical thickness is large implies

$$E_3|\tau_i-\tau_j| = \frac{1}{2} \qquad i = j$$

$$= 0 \qquad i \neq j$$

Using this relation it is readily seen that

$$F_i = \pi \int_\nu (J_{i+1}-J_i)d\nu$$

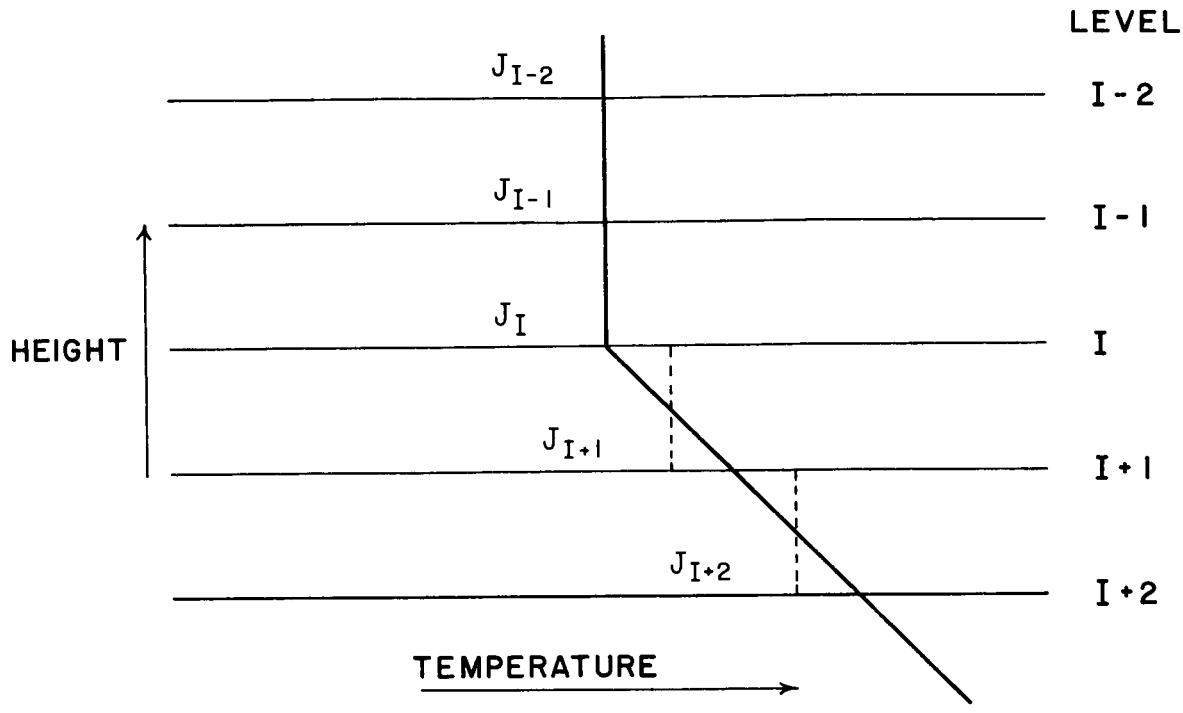

Fig. 1. Diagram of the source function as a function of height.

i.e., the flux at any level is proportional to $J_{i+1} - J_I$.

Thus

$$\begin{aligned} F_{I-2} &\alpha J_{I-1} - J_{I-2} = 0 \\ F_{I-1} &\alpha J_I - J_{I-1} = 0 \\ F_I &\alpha J_{I+1} - J_I > 0 \\ F_{I+1} &\alpha J_{I+2} - J_{I+1} > 0 \end{aligned} \qquad (2.6.2)$$

The heating at level i is proportional to $\Delta F_i = F_i - F_{i-1}$. Using these equations

$$\begin{aligned} \Delta F_{I-1} &= 0 \\ \Delta F_I &= J_{I+1} - J_I - J_I + J_{I-1} = J_{I+1} - J_I > 0 \\ \Delta F_{I+1} &= (J_{I+2} - J_{I+1}) - (J_{I+1} - J_I) \end{aligned}$$

The model correctly predicts no heating in level I-1, but produces a strong net heating in level I (the first layer in the isothermal region). The sign of the flux divergence in the I+1th depends on the relative sizes of J_I, J_{I+1} and J_{I+1}. By making layer I+1 small compared to layer I+2, the difference $(J_{I+2}-J_{I+1})$ can be made larger than $(J_{I+1}-J_I)$, producing a net heating in layer I+1. If however layer I+1 is small compared with layer I+2, the opposite effect can be produced and a net cooling is obtained.

This means that the isothermal layer assumption has two serious flaws.

(i) It tends to produce a greater amount of heating or cooling at the bottom of an isothermal layer in the atmosphere below which the temperature increases or decreases. This effect also occurs when the temperature gradient changes, not necessarily to an isothermal condition.

(ii) The sign of the flux divergence can be altered depending on the thickness of the slabs chosen.

It should be noted that even if the atmosphere is not optically thick in the region of the spectrum under consideration, these two errors still have a tendency to occur, although their effect is not so extreme. There are many regions of absorption spectra where the atmosphere is optically thick, at least near the line centers; an absorber in which this never happens has to be weak, and hence has to have little influence on the radiative transfer.

Clearly the isothermal layer approximation must not be used to study radiative transfer in important regions where the atmospheric temperature reaches a maximum or minimum (the tropopause, stratopause and mesopause),

and probably should not be used in other regions as well. A more realistic approach must be used, one which takes into account more accurately the structure of the atmosphere in the neighborhood of the point being investigated.

2.4.2 Polynomial Representation of the Source Function

Since the simplest approximation, that of isothermal layers, leads to serious errors in calculated flux divergences, a more sophisticated technique must be used. Perhaps the most obvious method is to express the source function at points within the individual layers as a polynomial in pressure or height or some other vertical coordinate. The isothermal layer approximation is really a limiting case, in which the degree of the polynomial is zero.

Suppose that the atmosphere has been divided into N horizontal plane-parallel layers, with the i-th layer bounded by pressure levels p_{i-1}, and p_i $(i = 1,2\ldots,N)$ with

$$0 = p_o < p_1 < \cdots < p_{i-1} < p_i \cdots < p_{N-1} < p_N = p_g$$

It will also be assumed that these levels have been chosen so that the atmosphere may, for the purpose of calculating atmospheric absorption, be approximated by homogeneous paths within the layers, as discussed in Section 2.3.2. For convenience, it will be assumed that $B(\nu,Tg) = J(\nu,\tau g)$. From Eq. (2.2.4) the expression for the net flux F_m at level m may be written.

$$F_m = 2\pi \int_\nu \{E_3(\tau_m)J(\nu,0) + \sum_{i=1}^{N} \int_{\tau_{i-1}}^{\tau_i} \frac{dJ}{dt} E_3(|t-\tau_m|)dt\}d\nu$$
$$(m = 0,1,\ldots,N) \qquad (2.4.3)$$

The assumption that the layers are homogeneous implies that within each layer t is a linear function of pressure, and that dJ/dt is a polynomial in p. Thus, each integral in the sum in Eq. (2.4.3) may be written

$$\int_{\tau_{i-1}}^{\tau_i} \frac{dJ}{dt} E_3(|t-\tau_m|)dt = \int_{p_{i-1}}^{p_i} \sum_{j=0}^{n-1} a_j\, p^j E_3(b_j+c_j p)\, dp \qquad (2.4.4)$$

where a_j, b_j, c_j are constants within the level i, and the source function is expressed as a polynomial of degree n in p, within level i.

Equation (2.4.4) can be evaluated using the relation (see appendix)

$$\int_{x_1}^{x_2} x^k E_n(x)\, dx = \sum_{j=0}^{k} \frac{(k)!}{(k-j)!} \left[x_1^{k-j} E_{n+1+j}(x_1) - x_2^{k-j} E_{n+1+j}(x_2)\right] \qquad (2.4.5)$$

This method is very similar to that proposed by Curtis (1956), in which the source function is expressed in terms of a polynomial of degree 4, whose coefficients are chosen to give the source function exactly at five adjacent levels. This representation is used only in the neighborhood of the point at which the flux divergence is being calculated, a lower order polynomial being used elsewhere. The higher order polynomial was used in an attempt to accurately include the contributions from nearby layers, which most influence the cooling rate in many parts of the atmosphere. This method was also used by Rodgers and Walshaw (1966).

The results of fitting such polynomials are shown in Fig. 2. The solid lines represent profiles typical of those encountered in standard or mean atmospheric profiles, while the dashed lines indicate the polynomial temperature distributions. Clearly the polynomials do not accurately represent the true profiles and may not give correct contributions to the cooling rate from adjacent layers. The polynomial frequently gives a smoother temperature profile, particularly where the temperature gradient is discontinuous and this property is sometimes desirable; the important modifying effect of such smoothing will be shown in the next chapter. Since a new polynomial is used for each point at which the cooling rate is calculated, no two points have, in general, the same temperature profile associated with them.

A further disadvantage of the higher order polynomials, at least for the method of calculation described here, is the difficulty in evaluating the integrals of the type in Eq. (2.4.5). Not only are they time consuming, but accuracy is difficult to maintain for some values of x_1 and x_2 due to roundoff errors and inaccuracies in calculating the exponential integrals.

The method applied here is to assume the source function is linear with pressure between adjacent pressure layers, and to simulate rapid temperature fluxuations by decreasing the thickness of the layers. The linear assumption enables Eq. (2.4.3) to be evaluated simply.

$$F_m = 2\pi \int_\nu \{E_3(\tau_m)J(\nu,0) + \sum_{i=1}^{N} \frac{\Delta J_i}{\Delta J_i} |E_4(|\tau_m-\tau_i|)-E_4(|\tau_m-\tau_{i-1}|)|\}d\nu \tag{2.4.6}$$

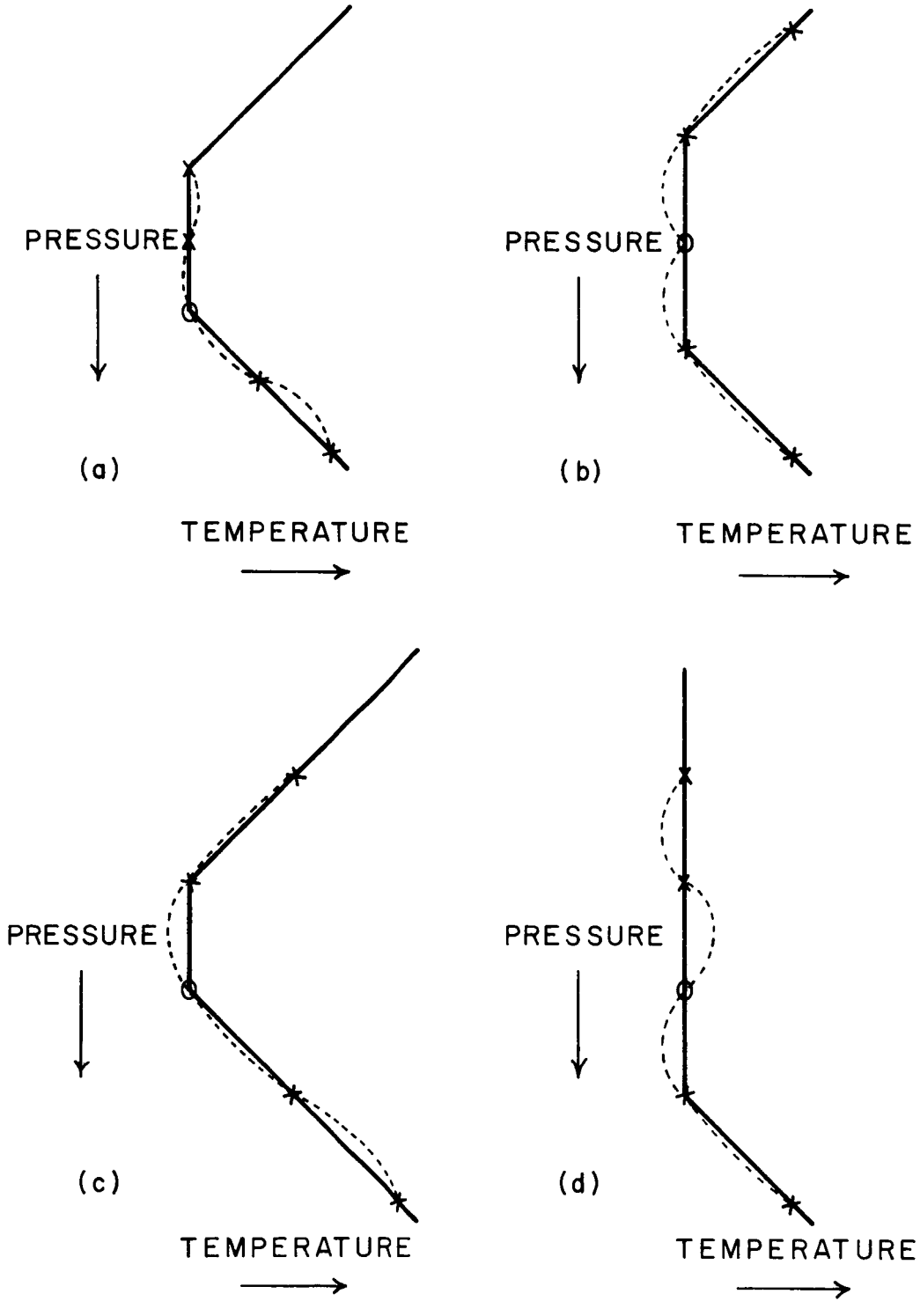

Fig. 2. Typical polynomial fits to vertical temperature structures. Circles mark pressure levels at which rate cooling is being determined; crosses mark other pressure levels at which polynomial gives exact source function. Solid line is temperature structure, dotted line is 4th degree polynomial fitting temperature structure.

where

$$\Delta J_i = J_i - J_{i-1}$$

and

$$\Delta \tau_i = \tau_i - \tau_{i-1}$$

In many molecular absorption bands, the source function J_i at level i is a slowly varying function of frequency, and may be considered constant over the band, or over some frequency subinterval of the band. For such a frequency interval Eq. (2.4.6) may be written

$$F_m = 2\pi\{J(\nu,0)[\int_\nu E_3(\tau_m)d\nu] + \sum_{i=1}^{N} \Delta J_i [\int_\nu \frac{1}{\Delta \tau_i} |E_4(|\tau_m - \tau_i|) - E_4(|\tau_m - \tau_{i-1}|)|d\nu]\}$$

i.e., the flux may be expressed as a linear combination of the source functions at all points in the atmosphere (c.f., Curtis, 1956). It should be noted that the coefficients in the linear sum are functions of temperature and strictly speaking should be used only for the atmospheric temperature structure for which they are calculated. In some spectral regions the coefficients are only weakly temperature dependent and may be used to calculate fluxes for other temperature structures, provided they are not radically different from the original.

As previously indicated, it is more difficult to compute flux divergences than fluxes, particularly in regions of the upper atmosphere where small flux differences cause large heating rates. For this reason

it is frequently advantageous to compute the divergence directly. Using Eq. (2.4.6) the flux difference at adjacent levels may be written

$$\begin{aligned}\Delta F_m &= F_m - F_{m-1} \\ &= 2\pi \int_\nu \{ [E_3(\tau_m) - E_3(\tau_{m-1})] J_o \\ &+ \sum_{i=1}^{m-1} \frac{\Delta J_i}{\Delta \tau_i} [(E_4(\tau_m - \tau_i) - E_4(\tau_m - \tau_{i-1})) - (E_4(\tau_{m-1} - \tau_i) - E_4(\tau_{m-1} - \tau_{i-1}))] \\ &+ \sum_{i=m+1}^{N} \frac{\Delta J_i}{\Delta \tau_i} [(E_4(\tau_{i-1} - \tau_m) - E_4(\tau_i - \tau_m)) - (E_4(\tau_{i-1} - \tau_{m-1}) - E_4(\tau_i - \tau_{m-1}))]\} d\nu \end{aligned} \tag{2.4.7}$$

Suppose that $\Delta\tau_i$ is small, for some i, and consider the errors which may arise in evaluating the terms in the sums in this equation. These terms involve differences of exponential integrals whose arguments differ by $\Delta\tau_i$. If $\Delta\tau_i$ is of the same order as the accuracy with which E_4 can be calculated, then the accuracy of calculating the difference will be relatively low. When the difference is divided by $\Delta\tau_i$ the absolute error in calculating the term becomes large, and test calculations showed that these errors often led to meaningless results.

Fortunately, it is not difficult to evaluate such terms with a much higher accuracy. The method is suggested by the mean value theorem

$$\frac{1}{\delta x} [F(x+\delta x) - F(x)] = F'(x+\zeta)$$

for some ζ in the range $0 < \zeta < \delta x$

Consider the errors involved in approximating $F'(x+\zeta)$ by $F'(x+\frac{1}{2}\delta x)$.

Expanding $F(x)$ and $F(x+\delta x)$ in a Taylor series

$$F(x+\delta x) = F(x+\tfrac{\delta x}{2}) + (\tfrac{\delta x}{2})F'(x+\tfrac{1}{2}\delta x) + \tfrac{1}{2!}(\tfrac{\delta x}{2})^2F''(x+\tfrac{1}{2}\delta x) + \tfrac{1}{3!}(\tfrac{\delta x}{2})^3F'''(x+\tfrac{1}{2}\delta_{\underline{x}})+O(\delta x)^4$$

$$F(x) = F(x+\tfrac{\delta x}{2}) - (\tfrac{\delta x}{2})F'(x+\tfrac{1}{2}\delta x) + \tfrac{1}{2!}(\tfrac{\delta x}{2})^2F'(x+\tfrac{1}{2}\delta x) - \tfrac{1}{3!}(\tfrac{\delta x}{2})^3F'''(x+\tfrac{1}{2}\delta x)+O(\delta x)^4$$

Subtracting

$$F(x+\delta x) - F(x) = \delta xF'(x+\tfrac{1}{2}\delta x) + \tfrac{1}{24}(\delta x)^3F'''(x+\tfrac{1}{2}\delta x) + O(\delta x)^5$$

Neglecting the terms of $O(\delta x)^5$

$$\frac{1}{\delta x}[F(x+\delta x)-F(x)] = F'(x+\tfrac{1}{2}\delta x) + \tfrac{1}{24}(\delta x)^2F'''(x+\tfrac{1}{2}\delta x) \qquad (2.4.8)$$

Applying this to the function $E_4(x)$

$$\frac{1}{\delta x}[E_4(x)-E_4(x+\delta x)] = E_3(x+\tfrac{1}{2}\delta x) + \frac{(\delta x)^2}{24}E_1(x+\tfrac{1}{2}\delta x)$$

The values of δx for which the approximation $E_3(x+\frac{1}{2}\delta x)$ should be used depends on the accuracy to which $E_4(x)$ can be calculated. The subroutines developed in the appendix give an absolute accuracy of approximately 1×10^{-7}. However, since adjacent values of the argument tend to have similar errors, the absolute error of the difference $[E_4(x) - E_4(x+\delta x)]$ is usually somewhat smaller.. But for some x and $x + \delta x$, particularly those that are computed from different polynomials, the error in the difference may be slightly more than 10^{-7}. It will therefore be assumed that an error of 10^{-7} is a representative value. The errors from the two methods

will become equal when

$$\frac{10^{-7}}{\delta x} \sim \frac{(\delta x)^2}{24} E_1(x)$$

Except for very small values of x, $E_1(x)$ is of order unity, so

$$\delta x \sim 10^{-2}$$

Using the approximation $E_3(x + \frac{1}{2}\delta x)$ for $\delta x < 10^{-2}$, the order of the error in computing

$$\frac{1}{\delta x} [E_4(x) - E_4(x + \delta x)]$$

is 10^{-5}, an acceptable value for the calculation of the flux divergences.

Using this approximation, the terms in the first sum of Eq. (2.4.7) become

$$\Delta J_i [E(\tau_m - \tau_{i-1/2}) - E(\tau_{m-1} - \tau_{i-1/2})]$$

where $\tau_{i-1/2}$ is defined as $(\tau_i + \tau_{i-1})/2$.
Further error can arise when $\Delta\tau_m$ is small, and can be treated in exactly the same way, reducing the term above to a still simpler form

$$-\Delta J_i \, \Delta\tau_m \, E_2(\tau_{m-1/2} - \tau_{i-1/2})$$

Inspection of Eq. (2.4.7) shows that the contribution from layer i to the flux differences in level m is the same, apart from a difference in sign and the multiplying factor $\Delta J_i/\Delta\tau_i$, as the contribution from layer m to the flux differences in layer i. This duality is of great importance, since the differences of the exponentials need be evaluated only once for

each i and m, which halves the execution time of this important part of the computer program.

It is also clear that the first term in Eq. (2.4.7) may, for small $\Delta\tau_m$, be approximated by

$$E_3(\tau_m) - E_3(\tau_{m-1}) \sim - \Delta\tau_m E_2(\tau_{m-\frac{1}{2}})$$

If the flux divergence at a point is required, the polynomial or linear approximation for the source function J may be substituted into Eq. (2.2.5), and integration with respect to t carried out in a similar manner.

Assuming that the atmosphere has been divided into horizontal layers in which the source function is a linear function of pressure, it is of interest to know how the flux divergence varies at points within these layers. Test calculations were made for layers as thin as 1 km. in the mesosphere, for the 15 μ CO_2 bands. It was found that the absolute value of the flux divergence was greatest near the boundaries of the layers and least near the center of the layers. The reason for this behavior is that at interior points the source function gradient is constant in the immediate neighborhood, whereas at the boundary it is usually discontinuous. The same problem undoubtably arises when a higher order polynomial is used; Fig. 2 shows that the source function gradient is not accurately reproduced. For example, in profile (b) the polynomial gives a local temperature maximum, which will tend to overestimate the cooling rate at that point. However, for temperature profiles which are smoother, the poly-

nomial may be more realistic. Nevertheless, if the flux divergence is calculated at a point, rather than an integrated value over a finite pressure layer, two important points must be taken into consideration.

(i) The method of calculation may distort the local temperature field and lead to inaccuracies.

(ii) The flux divergence at this point may not be representative of the value at neighboring points, and cannot in general be used as the average value in a finite pressure layer.

In the present study the thickness of layers was adjusted so that when a layer was halved and the flux differences recalculated the same values were obtained from the sum of the two sublayers, to within some acceptable error limits. The thickness of the layers depends on the accuracy required and on the characteristics of the spectral region under consideration. In the earth's mesosphere an accuracy of better than 1% can be obtained in the 15 μ CO_2 bands with layers several km thick.

The integrations with respect to frequency of equations such as Eq. (2.4.7) can be carried out in much the same way as those developed for calculating transmissivity (Drayson & Young 1966). The frequency interval of integration is divided into many subintervals, whose length varies, being smallest near line centers and largest away from lines, and 4-point Gaussian quadrature is applied over the intervals.

2.5 CONCLUSIONS

In deriving the equations of radiative transfer and manipulating

them into a form suitable for numerical evaluation of flux divergences, a concerted effort has been made to use as few approximations as possible. As a result several approximations, almost universally employed, have been avoided. This is not meant to imply that these approximations are valueless, but that under some circumstances they may lead to errors and must be used with caution. The more exact methods can provide a means to check the approximations and define some conditions under which they can be employed. Flux divergences are obtained by direct integration with respect to frequency. The assumption that the source function is linear in pressure within the atmospheric layer is shown to have advantages over the use of isothermal layers and higher order polynomials, and also allows the vertical integration to be accomplished simply, without the use of a diffusivity approximation for angular integration.

The disadvantage of the present method is that the formulation is rather complicated, and that quick simple solutions cannot be obtained. A considerable amount of computing time is required to solve any realistic problem. However, with computers of increasing speed, the time problem should steadily decrease.

Apart from checking other methods, calculations of this type can be justified only if they result in considerable improvement over faster, simpler techniques. The next two chapters are devoted to two applications, with emphasis on comparison with other calculations.

CHAPTER 3

APPLICATION TO THE EARTH'S MESOSPHERE AND MESOPAUSE

3.1 GENERAL SURVEY OF LONG-WAVE RADIATIVE TRANSFER IN THE EARTH'S ATMOSPHERE

In the earth's atmosphere the important gases for long-wave radiative transfer are minor constituents (with the possible exception of atomic oxygen in the thermosphere), comprising much less than 1% of its mass. Of these, the most influential are:

(a) Carbon dioxide. CO_2 is a linear symmetric molecule which has no pure rotational spectrum. The important bands for infrared radiative transfer are as follows.

(i) The 15 μ bands, consisting of the ν_2 fundamental and overtone bands. In addition to the normal molecule ($^{12}C\ ^{16}O\ ^{16}O$), the isotopic species $^{13}C\ ^{16}O\ ^{16}O$, $^{12}C\ ^{16}O\ ^{18}O$, $^{12}C\ ^{16}O\ ^{17}O$ and $^{13}C\ ^{16}O\ ^{18}O$ are abundant enough to exert some influence. The last three are asymmetric.

(ii) The ν_3 fundamental at 4.3 μ.

Although the ν_3 band intensity is much greater than the total intensity of the bands near 15 μ, it plays only a minor role in the earth's atmosphere because the thermal energy is low near 4.3 μ at atmospheric temperatures.

(b) Water vapor is a nonlinear molecule with two important atmospheric absorption bands.

(i) The pure rotational band, with lines distributed from the micro-wave region to 20 μ. Between 10 and 20 μ the absorption is due partly to weak absorption lines in the interval and partly due to the wings of distant lines.

(ii) The ν_2 band near 6.3 μ. Again the wings of lines in this band gives considerable absorption at least out to 10 μ.

Lines of isotopic molecules are again important.

(c) Ozone is also an asymmetric molecule with complicated band structures. The two important absorption regions are:

(i) The 9.6 μ bands, which consist of two bands, the ν_1 and ν_3 fundamentals, centered at 1110 cm^{-1} and 1043 cm^{-1} respectively.

(ii) A weaker 14 μ band, identified as the ν_2 band.

For each molecule there are many more molecular absorption bands in the infrared but these are either too weak or occur at frequencies which are too high to influence the long-wave radiative transfer. Similarly, some of the even less abundant atmospheric constituents e.g., CH_4, N_2O have strong absorption bands, but their mixing ratio in the atmosphere is so low that they do not contribute significantly to atmospheric radiative transfer.

To apply the methods developed in the previous chapter it is essential to know the frequency, intensity and Lorentz half-width of the absorption lines. As indicated eariler, a sound knowledge of the band structure is

often lacking, even for the common atmospheric absorbing molecules. The state of knowledge of these bands outlined above will now be examined.

(a) Carbon dioxide. The linearity of this molecule makes it comparitively easy to handle theoretically and the line positions and relative intensities of the individual bands can be readily calculated.

(i) The 15 μ bands. These important bands have been intensively studied, both theoretically and experimentally. Although the structure of the individual bands is simple, their overlapping makes it difficult to determine the relative intensities of the bands, and even the total band intensity. Knowledge of variation of Lorentz half-width with rotational quantum number is incomplete, particularly for air or nitrogen broadening. Despite these difficulties theoretical calculations show good agreement with laboratory spectra (Drayson et al., 1967) and atmospheric radiances (Chaney et al., 1967)

(ii) The 4.3 μ bands. The somewhat simpler structure of these bands make this region easier to investigate, and satisfactory agreement between theoretical and experimental data exists (Gray, 1965). Larger errors can be tolerated in this spectral region, since the thermal energy is low at atmospheric temperatures.

(b) Water vapor is a non-linear molecule which has been investigated intensively in recent years.

(i) The pure rotational band. Line positions, intensities and Lorentz half-widths have been calculated by Benedict and Kaplan. Qualitative agreement with experimental data is good, although the amount of absorption is not always identical. The use of modified line shapes, in particular the Van Vleck-Weisskopf line shape, may lead to improvement, particularly in the region between 10 and 20 μ.

(ii) The 6.3 μ band. This band has received comparatively little theoretical investigation and results are inconclusive at the present time.

(c) The theoretical and experimental difficulties of determing water vapor absorption apply even more to ozone. The difficulties and dangers of generating the gas have detered most investigators, and for many years some of the bands were incorrectly identified. Quantitative measurements have been made by Walshaw (1957) and by McCaa & Shaw (1967).

(i) The 9.6 μ bands. Line positions and intensities in this region have been calculated by Kaplan (1956) and by Clough and Kneizys (1965); unfortunately neither gives agreement with experimental spectra. More work is required on this extremely difficult molecule.

(ii) The 14 μ band has been measured quantitatively for the first time by McCaa and Shaw (1967). No theoretical work has been published.

Thus, at the present time the 15 μ bands of carbon dioxide are best understood. The distribution of carbon dioxide with altitude has been measured frequently and the results show that the mixing ratio is approximately constant, except close to the surface. (Bolin and Keeling 1963). These are small variations with latitude and nearness to land masses, as well as a slow increase with time. This presumably holds true up to the altitude where carbon dioxide begins to dissociate at about 100 km, although no measurements are available to support this supposition. In the stratosphere, mesosphere and mesopause regions, carbon dioxide is the principal absorber of lone-wave radiation; in the troposphere its relative role gradually decreases and is dwarfed by water vapor near the surface (Möller, 1963).

The distribution of water vapor is extremely variable and is not known with any certainty above the tropopause (Newell, 1967). Whatever its distribution, it is very important in the troposphere, particularly near the surface, and less important at higher altitudes. The influence of the 6.3 μ water vapor band is small compared to that of the rotational band (Kuhn, 1966).

The situation as regards ozone is discouraging. The atmospheric absorption in the 14 μ band is weak and is masked by the strong absorption of the 15 μ CO_2 bands. The 9.6 μ atmospheric absorption is moderately strong and falls in an otherwise largely transparent region of the spectrum. Calculations by Plass (1956a) and Kuhn (1966) indicate that it provides an important cooling mechanism in the upper stratosphere,

falling off quite rapidly above and below this level.

In the remaining part of this chapter the cooling due to the 15 μ bands carbon dioxide in the mesosphere, mesopause and lower thermosphere will be investigated. It is clear from the preceding discussions that this is the dominant band at these altitudes, as well as being the one with the best understood structure. In addition the concentration of CO_2 is better known than O_3 or water vapor. Moreover, recent results (Kuhn 1966, Kondrat'yev et al., 1966) have indicated that CO_2 is responsible for some atmospheric heating at the mesopause level and the calculations to be described were designed to confirm or reject these results. A point of further interest lies in the evaluation of a source function in the mesopause and lower thermosphere, where significant deviations from the Planck black body function occur.

3.2 EQUATIONS FOR THE SOURCE FUNCTIONS IN THE UPPER ATMOSPHERE

For a gas that is in thermodynamic equilibrium it is well known that the source function is given by the Planck black-body function

$$B(\nu,T) = 2h\nu^3/c^2[\exp(h\nu/kT)-1] \qquad (2.2.1)$$

where

h is the Planck constant

k is the Boltzmann constant

c is the velocity of light in vacuum

and

T is the absolute temperature

In the atmosphere, where radiative heating or cooling is taking place, strict thermodynamic equilibrium is not maintained and the source function is not equal to the Planck function. However, for much of the earth's atmosphere the deviation from the Planck function is slight, and the fluxes may be calculated from the equations of the previous chapter, assuming equality between the two functions.

Near the mesopause, however, for the 15 μ CO_2 bands the differences become larger and the errors induced by assuming equality become serious (Curtis and Goody 1956). The explanation for the breakdown is as follows: for a CO_2 molecule in thermodynamic equilibrium the vibrational energy is distributed over the vibrational states according to a Boltzmann distribution. In the non-equilibrium case, the Boltzmann distribution is disturbed by the gain or loss of radiant energy. If molecular collisions are sufficiently frequent the vibrational energy regains its Boltzmann distribution by loss or gain from translational energy. However, there is a possibility that an excited molecule may re-emit its energy before the equilibrium process can be completed. These two mechanisms are characterised by two time constants, the former being the relaxation time λ, the latter the radiative life-time θ. The same is true for the rotational energy states.

If $\lambda \ll \theta$, a distribution close to the Boltzmann distribution is attained and the Planck function becomes a good approximation. Conversely if $\theta \ll \lambda$ very little collisional exchange of energy will occur and the

atmosphere will act as pure scattering atmosphere. Between these two extremes both processes are important and some alternative form for the source function must be found. The problem is complicated because the source function depends on the radiation field, which in turn depends on the source function.

Laboratory measurements have shown that the rotational relaxation time is approximately three orders of magnitude less than the vibrational relaxation time of the ν_2 CO_2 band, so that levels where vibrational relaxation begins to become important a Boltzmann distribution over the rotational energy levels may still be assumed. Rotational relaxation never becomes important in the earth's atmosphere, because the molecule is dissociated at the level around 120 km where the radiative lifetime and the rotational relaxation time would become comparable (Curtis and Goody, 1956).

The first derivation of an equation for the source function in the earth's upper atmosphere for the 15 μ CO_2 bands was made by Curtis and Goody (1956), in a paper that has become a classic in the field. They assumed a simple harmonic oscillator model in which the rotational energy levels have a Boltzmann distribution. The equation of radiative transfer was written in terms of Einstein transition probability coefficients and related to the number density of vibrational quanta, E. The transfer of energy between the vibrational and translational modes was taken into account by use of the equation

$$\frac{dE}{dt} = -\frac{1}{\lambda}(E - \bar{E}) \qquad (3.2.2)$$

where $\bar{E}$ is the value of E when the vibrational energies have a Boltzmann distribution. The final form of the equation relating the flux divergence and the source function is

$$\frac{dF}{du} = \frac{4\pi S\Theta}{\lambda}(J - B) \qquad (3.2.3)$$

where S is the band intensity.

Kuhn (1966) derived the source function in a rather different way, analogous to the two level atom problem in astrophysics. He determined the ratio of the populations of the 0 and 1 energy levels of the CO_2 molecule and showed further that the influence of a third level could be neglected for carbon dioxide in the earth's upper atmosphere. The derived equation is identical to that of Curtis and Goody, expressed in Eq. (3.2.3).

An equation for the source function has also been obtained by Shved (1965a), using gas kinetic equations, and takes the form

$$J = B\left[1 + \frac{g_o}{g_1}\frac{H\lambda\exp(h\nu_o/kT)}{N}\right] \qquad (3.2.4)$$

where

ν_o is the frequency of the band center,

g_o and g_1 are the statistical weights of the lower and upper levels respectively,

H is the flux divergence in quanta cm^{-3} sec^{-1}

and

N is the number density of absorbing molecules.

This expression apparently has a different form from Eq. (3.2.3) but can be changed using the approximation

$$B(\nu,T) \sim \frac{2h\nu_o^2}{c^2} \exp(-h\nu_o/kT) \qquad (3.2.5)$$

This approximation is used in all three derivations and introduces a maximum error of about 2% in B. Shved's Equation (3.2.3), becomes

$$\frac{dF}{du} = \frac{h\nu_o H}{N} = \frac{g_1}{g_o}\frac{1}{\lambda}\frac{c^2}{2\nu_o^2}(J-B) \qquad (3.2.6)$$

The radiative lifetime θ is related to the total band intensity S by the following equation

$$\theta^{-1} = 8\pi \frac{g_o}{g_1}\frac{\nu_o^2}{c^2} S \qquad (3.2.7)$$

(Mitchell and Zermansky 1934, Penner 1959). Substituting into Eq. (3.2.3), Eq. (3.2.6) is obtained, i.e., the same equation for the source function is obtained in each of the three cases. It should be noted, however, that both Curtis and Goody, and Kuhn neglected to include the factor of the ratio of statistical weights in Eq. (3.2.7). For the CO_2 fundamental, $g_1 = 2g_o$, so that the final equations are in error by a factor of 2. This is equivalent to using vibrational relaxation times of twice the nominal values quoted in their papers. When referring to their results this correction will be automatically applied. Although a factor of two appears to be an important quantity the uncertainty of an order of magnitude in the relaxation time λ prevents a more accurate determination of flux divergence, as dis-

cussed later. The methods of deriving the equation for the source function employed by Shved and Kuhn are basically the same, and are also contained in Kondrat'yev (1965). They do not depend on the simple harmonic oscillator model used by Curtis and Goody; the latter represents a simplication of the energy states of the molecule, but retains many essential features, so that the equations obtained in each derivation are identical.

A rather large number of assumptions and approximations in addition to those already mentioned have been made in the derivations of equations. The more important of these are:

(i) It has been assumed that, in the regions of the atmosphere where deviations from Kirchoff's law become important, the lines of the individual bands are non-overlapping. This presents no difficulty since the lines in the earth's mesosphere and above are very narrow, and no appreciable overlap occurs, even in the Q-branches where the spacing is least.

(ii) The source function $J(\nu,T)$ has been approximated by $J(\nu_o,T)$, where ν_o is the center of the band, i.e., it has been assumed independent of frequency within the confines of the band. In particular this implies that the Planck function is replaced by a frequency independent function over these frequencies. Fortunately, the Planck function varies slowly with frequency in the 15 μ region at mesospheric temperatures. However, the effect on the accuracy of the calculations is difficult to assess. It is better to look on this approximation as one which makes the calculation possible at this time and accept it until a more complete solution can be found.

(iii) The equations apply to a single band only, and then only to the fundamental. This fact has some important implications.

(a) The equations cannot be applied to the weaker overtone bands, some of which are important in and above the mesosphere.

(b) The equations are valid for the fundamentals of the molecules with the less common carbon and oxygen isotopes. These molecules play a much more important role in radiative transfer than their relative abundance would suggest. The overtone bands of these isotopes are not significant.

(c) Where local thermodynamic equilibrium breaks down there is no single source function applicable to all bands, but a different one must be derived for each individual band. In general, the level at which deviations from the Planck black-body function become significant will vary from band to band, and will be expanded upon later. Using Eq. (3.2.1) and (2.1.6) the expression for the source function becomes

$$J - B = \frac{g_1}{g_o} \lambda \frac{2\nu_o^2}{c^2} \, 2\pi \int_\nu \int_{-1}^{+1} [I(\nu,\tau,\mu) - J(\nu,\tau)] k_\nu \, d_\mu \, d_\mu \tag{3.2.8}$$

The dependence on the ratio λ/Θ has now reappeared since the absorption coefficient k_ν in the integrand is proportional to the band intensity S and therefore proportional to $1/\Theta$. This means that the source function for the band is determined solely by the ratio λ/Θ and the atmospheric structure parameters, all other quantities being constant for the band.

To obtain the flux divergence the source function is evaluated from Eq. (3.2.8). In Section 2.4.2 it was shown that the integral could be expressed as a linear sum of source functions at all levels in the atmosphere. At each level i the source function can be expressed as

$$J_i - B_i = \sum_{j=1}^{N} \alpha_{ij} J_j \quad i = 1,2,\ldots,N \qquad (3.2.9)$$

This set of N linear simultaneous equations may be solved for the N unknowns $J_1,\ldots,J_N$. The solution presents no particular numerical difficulty, at least in the cases encountered in the calculations made here. A double back substitution method was employed, using a library subroutine of the University of Michigan Computing Center. Another subroutine (a Gauss-Jordan reduction with a complete pivotal strategy) gave almost identical results.

The flux divergence may be evaluated from Eq. (3.2.6) or Eq. (2.1.6), once the source functions have been obtained. Using both equations provides a good check on the accuracy of solution of the linear equations. The heating rates obtained from the two equations were very close, except at high pressures, where λ is small. Under these conditions J and B are almost identical, i.e., local thermodynamic equilibrium exists, and the accuracy with which the numerical value of these functions can be represented in the computer produces a large relative error in their difference. It is better to calculate flux divergence using Eq. (2.1.6) at high pressures.

For the reasons outline in Section 2.4.2 the finite difference for-

mulation of the flux divergence is preferred and Eq. (2.4.6) is used in place of Eq. (2.1.6). The flux divergence in the ith layer is assumed to be that of the mid point where, because of the linearity of J and B, the source function and Planck function have a value equal to the average of the values at the boundaries. The system of linear Equations (3.2.11) is replaced by a slightly modified system in the form

$$\frac{J_i + J_{i-1}}{2} - \frac{B_i + B_{i-1}}{2} = \sum_{j=1}^{N} \alpha_{ij} \left(\frac{J_j + J_{j-1}}{2} \right) \qquad i = 1,2,\ldots,N \tag{3.2.10}$$

This number of unknowns is now N + 1, with only N equations to determine them. A further condition is that at the surface the source function is identical to the Planck function, i.e.,

$$B_N \equiv J_N$$

In the earth's atmosphere no difficulty arises from this assumption because almost any reasonable value of J_N leaves the cooling in the upper atmosphere unchanged. Otherwise the solution proceeds in exactly the same way.

The equations for the source function have been derived on the assumption that the absorption lines in the mesosphere and above are non-overlapping. In the mesosphere Doppler broadening dominates the line s shape, where the Doppler half-width is approximately 6×10^{-4} cm^{-1}. The region of the 15 μ CO_2 bands near 668 cm^{-1} has the highest line density,

containing the Q-branches of the $^{12}C^{16}O_2$ fundamental and some overtones. The line spacing is approximately 1×10^{-2} cm^{-1}, so that non-overlapping is a valid assumption. In the mesosphere much of the incident radiation field orginates from the troposphere where overlapping is important. Nevertheless, the flux divergence at the upper levels can be accurately computed on the assumption that the lines are non-overlapping throughout the atmosphere. In Eq. (2.1.6) the expression for flux divergence contains the weighting factor k_ν in the integrand; away from the line centers k_ν is zero, but near the line center, where k_ν is large, the absorption is complete well above the levels where overlapping is significant, unless the line is extremely weak and ineffective in radiative transfer. (Cf. Shved, 1964).

3.3 CALCULATION DETAILS

For each absorption band in the mesosphere, the total flux divergence was expressed as the sum of the flux divergences for the individual lines. In each of the P, Q and R branches of the bands, variations from line to line were found to be small, so that calculation of every third rotational level provided sufficient accuracy with a considerable saving in computing time.

The most uncertain parameter is the vibrational relaxation time λ. Experimentally it is difficult to determine, especially for the temperatures encountered near the mesopause and theoretical estimations of λ do not produce agreement with experimental data. A complete discussion, in-

cluding the possible catalytic effect of water vapor is given by Shved (1965a). The value of λ probably lies within the range 2×10^{-6} to 2×10^{-5} sec at 1 atmosphere and about 200°K. Since the relaxation time depends on the frequency of molecular collisions, λ is inversely proportional to pressure p.

After the cooling rate calculations had been made, a paper by Read (1965) was brought to the author's attention. The vibrational relaxation time for CO_2-CO_2 collisions is approximately 6×10^{-6} sec at 1 atm and 280°K. The values used here (between 2×10^{-6} and 2×10^{-5} secs) bracket this result. The presence of small amounts of water vapor significantly reduces the relaxation time. The values for CO_2-N_2 collision is not given.

The concentration of carbon dioxide was assumed to be constant up to 120 km at .314 per cent by volume, but the calculated heating rates are not sensitive to small changes. CO_2 starts to dissociate at about 100 km (Curtis and Goody, 1956) so that radiative heating rates above this level are uncertain. The effect on heating rates lower in the atmosphere is unimportant, as shown by test calculations.

Because the primary interest in this calculation was on the behavior near the mesopause, thin layers were used between 70 and 90 km (about 2 km), and rather thicker layers elsewhere (5 km in the thermosphere and mesosphere). Layers of 5 km. thickness in the region of the mesopause were found to distort the cooling rates at these levels.

The band parameters (line positions, intensities and Lorentz half-width) used in the calculations are taken from Drayson and Young (1966)

and Drayson et al., (1967). Table I lists all the bands which are important at atmospheric temperatures. The most common of the CO_2 molecules are given in Table II, with their abundance relative to $^{12}C^{16}O_2$. The value of the Lorentz half-width used was 0.08 cm^{-1} at 1 atm and 300°K. This value is somewhat uncertain, but at mesopheric pressures the lines are predominantly Doppler broadened, and errors in the Lorentz half-widths are not significant.

The intensities of the weak bands in the 15 μ region are also uncertain, particularly those which are overlapped by strongly absorbing bands. However, their role in radiative transfer near the mesopause is small, largely a result of their rapid decrease in intensity with decreasing temperature. This point will be discussed more fully when the results of the calculations are presented.

3.4 RESULTS OF CALCULATIONS AND COMPARISON WITH PREVIOUS RESULTS

3.4.1 Cooling Rates for Model Atmospheres

Radiative transfer calculations are frequently applied to standard or model atmospheres, which are important because they represent average temperature profiles and are not encumbered with fine structural details. Many radiative transfer models are not capable of representing such fine structure and this provides an additional reason for using the smooth profiles.

The calculations for the U. S. Standard Atmosphere (1962) demonstrate many of the features common to all model atmospheres at the mesosphere

TABLE I

BAND INTENSITIES USED IN CALCULATING ROTATIONAL LINE INTENSITIES
(From Drayson et al., 1967)

	Level		Band Center	Intensity
	Lower	Upper	($^{12}C\ ^{16}O_2$)	(cm^{-1}(atm cm)$^{-1}$ at 300°K)
1	000:0	010:1	667.379	194
2	010:1	020:0	618.033	4.27
3	010:1	100:0	720.808	6.2
4	010:1	020:2	667.750	15.0
5	020:0	030:1	647.054	1.0
6	020:0	110:1	791.447	0.022
7	020:2	030:1	597.337	0.14
8	020:2	110:1	741.730	0.14
9	020:2	030:3	668.151	0.85
10	100:0	110:1	688.672	0.3
11	100:0	030:1	544.279	0.004
12	030:3	040:2	581.62	0.0042
13	030:3	120:2	757.47	0.0059
14	030:1	120:2	828.284	0.00049
15	030:1	120:0	738.364	0.014

TABLE II

RELATIVE ABUNDANCE OF ISOTOPIC MOLECULES
(From Drayson and Young, 1966)

	Molecule	Abundance Relative to $^{12}C\ ^{16}O_2$	Band Center Of Fundamental
0	$^{12}C\ ^{16}O_2$	1.00	667.4
1	$^{13}C\ ^{16}O_2$	1.12×10^{-2}	648.5
2	$^{12}C\ ^{16}O^{18}O$	4.0×10^{-3}	662.3
3	$^{12}C\ ^{16}O\ ^{17}O$	8.0×10^{-4}	664.7
4	$^{13}C\ ^{16}O\ ^{18}O$	4.5×10^{-5}	643.6

and mesopause levels. The equations for the fundamental transition, described in the previous section, were applied to each of the isotopes separate using values of the vibrational relaxation time $\lambda_o = 2 \times 10^{-6}$, 4×10^{-6}, 10^{-5} and 2×10^{-5} sec, where λ_o is the value of λ at 1 atmosphere. It was found that only isotopes 0, 1, 2, and 3 (Table II) gave any contribution to radiative transfer in the upper atmosphere (greater than about 0.1°K per day heating or cooling). The full results are too extensive to give here in detail; only representative values will be given. The cooling rates for the four bands are shown in Table III for the value $\lambda_o = 1 \times 10^{-5}$ sec. Table IV provides details of the deviation of the source function from the black body function. For isotope 0 the deviation does not become apparent until about 80 km, while for isotope 3 the difference begins near the stratopause. It is interesting to note that at that level the radiative lifetime θ is still approximately two orders of magnitude greater than the relaxation time λ, a condition generally unfavorable for vibrational relaxation. The reason can be explained by rewriting Eq. (3.2.6) in the form

$$\frac{dF}{dp} = \frac{dF}{du}\frac{du}{dp} = \frac{du}{dp}\frac{g_1}{g_o}\frac{1}{\lambda}\frac{c^2}{2\nu_o^2}(J - B)$$

$\frac{du}{dp}$ is proportional to the mixing ratio, which is very small for the less abundant isotopes. This implies that large differences between the source function and the Planck function are required before appreciable cooling can occur.

TABLE III

COOLING RATES IN ^{o}K/DAY FOR THE INDIVIDUAL BANDS,
U.S. STANDARD ATMOSPHERE (1962), $\lambda_o = 1 \times 10^{-5}$ SEC

Height (km)	Iso. Band	0 1	1 1	2 1	3 1	0 2	0 3	0 4
107.5		3.01	.03	.00	.00	.92	.66	1.01
102.5		3.80	.03	.01	.00	.60	.43	.89
97.5		4.67	.03	.00	.00	.18	.09	.45
92.5		5.03	.01	-.02	-.01	-.05	-.11	.04
89.0		3.49	-.03	-.05	-.01	-.12	-.17	-.26
87.0		3.25	-.05	-.07	-.02	-.13	-.17	-.28
85.0		2.48	-.08	-.10	-.02	-.13	-.18	-.30
83.0		1.33	-.13	-.14	-.03	-.14	-.18	-.33
81.0		-.16	-.20	-.18	-.04	-.15	-.19	-.37
79.0		-.45	-.23	-.21	-.05	-.14	-.19	-.35
77.0		.30	-.17	-.19	-.04	-.09	-.16	-.21
75.0		.55	-.09	-.16	-.04	-.02	-.09	.00
73.0		.68	.00	-.10	-.02	.09	.00	.26
71.0		.81	.11	-.02	.00	.21	.12	.55
68.0		.86	.26	.12	.04	.37	.29	.88
64.0		1.36	.45	.34	.11	.60	.56	1.33
60.0		1.89	.50	.48	.16	.62	.62	1.34
56.0		2.40	.44	.52	.20	.51	.53	1.11
53.0		3.02	.45	.55	.21	.53	.55	1.19
49.5		3.23	.39	.47	.21	.45	.46	1.07
44.0		2.85	.31	.30	.15	.34	.33	.85

TABLE IV

RATIO J/B FOR INDIVIDUAL BANDS, U.S. STANDARD ATMOSPHERE (1962), $\lambda_o = 1 \times 10^{-5}$ SECS

Height (KM)	Iso. Band	0 1	1 1	2 1	3 1	0 2	0 3	0 4
110		.07	.27	.42	.45	.45	.39	.31
105		.13	.38	.61	.67	.71	.65	.50
100		.20	.59	.95	1.05	.93	.92	.77
95		.40	.81	1.32	1.47	1.00	1.02	.99
90		.72	1.18	1.89	2.10	1.01	1.04	1.04
88		.80	1.18	1.86	2.07	1.01	1.03	1.03
86		.89	1.21	1.82	2.00	1.01	1.02	1.02
84		.95	1.21	1.77	1.94	1.01	1.01	1.02
82		.99	1.24	1.77	1.83	1.00	1.01	1.01
80		1.01	1.24	1.64	1.74	1.00	1.01	1.01
78		1.00	1.12	1.34	1.39	1.00	1.00	1.00
76		1.00	1.04	1.18	1.21	1.00	1.00	1.00
74		1.00	1.01	1.07	1.08	1.00	1.00	1.00
72		1.00	.99	1.03	1.02	1.00	1.00	1.00
70		1.00	.99	.99	.98	1.00	1.00	1.00
66		1.00	.99	.98	.96	1.00	1.00	1.00
62		1.00	.99	.98	.97	1.00	1.00	1.00
58		1.00	1.00	.99	.98	1.00	1.00	1.00
54		1.00	1.00	.99	.99	1.00	1.00	1.00
52		1.00	1.00	1.00	.99	1.00	1.00	1.00
47		1.00	1.00	1.00	1.00	1.00	1.00	1.00

This result is important for the radiative transfer in upper levels of other planetary atmospheres. In Mars and Venus for example carbon dioxide is a major atmospheric constituent and vibrational relaxation of the fundamental will not take place until lower pressures are reached, possibly not until dissociation takes place, at least for the isotope $^{12}C\ ^{16}O_2$.

The equations for vibrational relaxation have not been derived for overtone bands. Nevertheless the equations developed for the fundamental were applied to these bands. It was found that only the three strongest overtones were important for radiative transfer in the upper mesosphere and moesopause region (bands 2, 3 and 4) and these only for the molecule $^{12}C\ ^{16}O_2$. For these bands the ratio of the statistical weights is unity. Furthermore, relaxation is not significant even at 80 km, as can be seen from Table IV.. This is due, in part at least, to the fact that the radiative lifetime of these weaker bands is at least 1 to 2 orders of magnitude larger than the fundamental. Because the bands are relatively weak, the magnitude of the heating and cooling rates is quite small. Unless the equations for vibrational relaxation are in a quite different form for these bands, or the vibrational relaxation time λ is much larger than for the fundamental, the method of calculation should introduce only a small error.

The total cooling for all bands for the U. S. Standard Atmosphere, (1962) is shown in Fig. 3, for values of $\lambda_o = 2 \times 10^{-6}$, 10^{-5} and 2×10^{-5} sec and are compared with the values of Kuhn (1966). For all values of

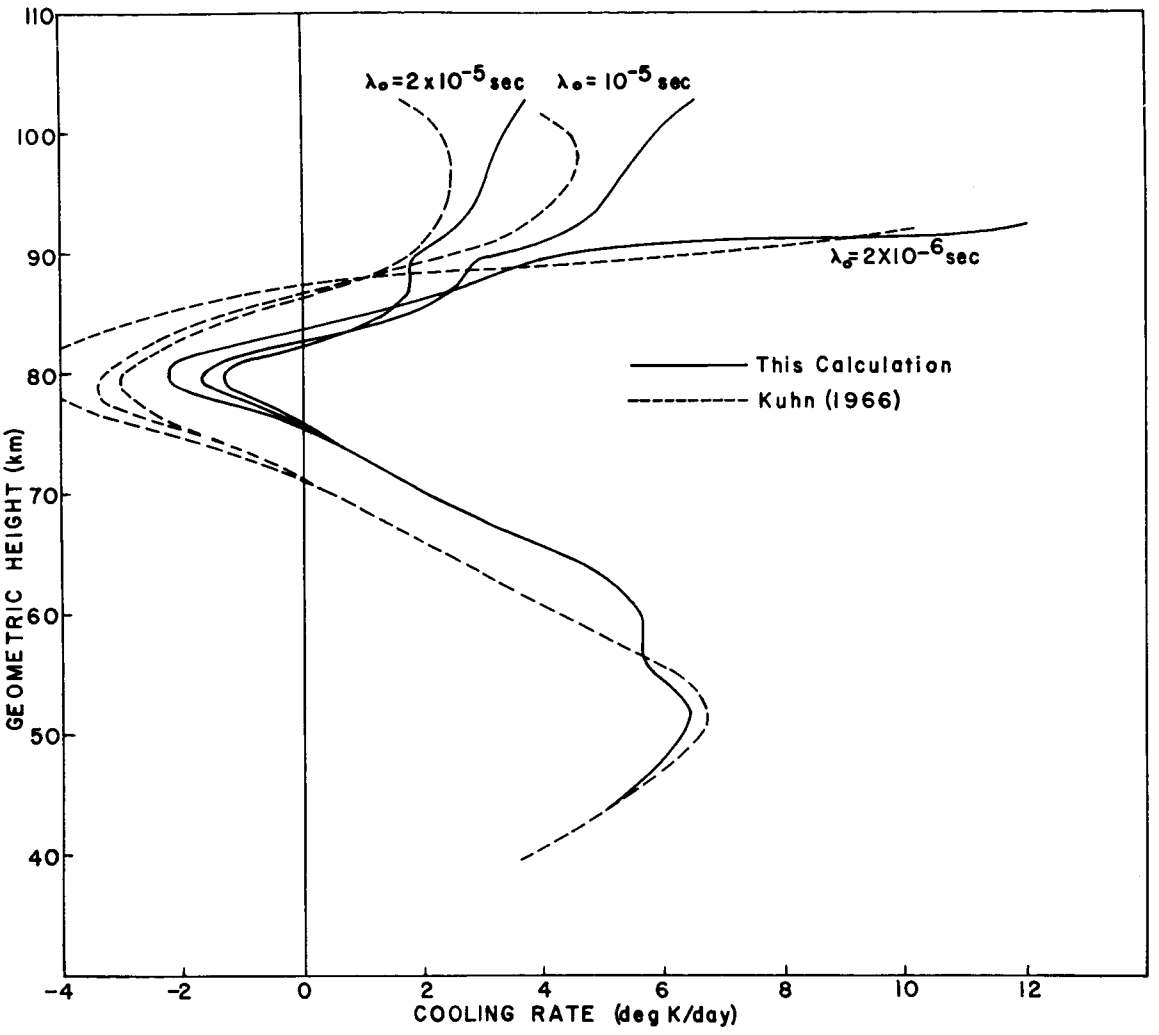

Fig. 3. Calculated cooling rates for the U.S. Standard Atmosphere (1962).

λ_o the present calculations show a small amount of heating near the base of the mesopause, although its magnitude and vertical extent are both significantly smaller then those of Kuhn. In the thermosphere the present results show much more cooling. This is a consequence of the separate relaxation of the bands, since the weak overtone bands are not completely relaxed, even at 110 km. and have appreciable contribution to cooling at this level. Near the stratopause the assumption of non-overlapping lines may begin to break down and some of the weaker bands also provide an appreciable source of cooling. The present calculations were not designed to be accurate in this region of the atmosphere.

There are a number of important differences between the two methods of calculation. Kuhn's calculations included the following features:

(a) Isothermal layers were used

(b) Equation (3.2.6) was applied to the total flux divergence for all bands, i.e., the bands were not relaxed separately.

(c) A constant temperature was used to calculate line intensities in the mesosphere.

(d) The quasi-random band model was used.

It has already been shown that (a) tends to produce greater heating at a temperature minimum. Test calculations showed that (c) exhibited the same tendency. Because the lines are isolated in the mesosphere the redistribution of the lines by the model does not change the absorption and (d) does not contribute errors directly.

Test calculations were made to determine the effect of (b). The differences in cooling rates were greatest for the larger values of λ_o, the new calculation giving an additional heating of about 0.4 deg k/day near 80 km for $\lambda_o = 2 \times 10^{-5}$, but only half this value for $\lambda_o = 2 \times 10^{-6}$ sec. In the lower thermosphere the effect was more pronounced, roughly having the cooling rates above 100 km. Calculated in this way, the cooling rates in the lower thermosphere are in good agreement with Kuhn, but the differences in the mesosphere and at the mesopause are virtually unchanged.

One of the effects of atmospheric long wave radiative transfer is to smooth discontinuities in temperature gradient, and tends to produce a maximum of heating or cooling where such discontinuities exist. Many model atmospheres, including the U. S. Standard Atmosphere (1962), contain such features. A calculation was made for this atmosphere, with the temperature structure smoothed at the base of the mesopause, where heating was previously obtained. The new cooling rates are shown in Fig. 4. The heating has been very much reduced (about 0.6 deg K/day maximum) or entirely eliminated, depending on the value of λ_o. In view of the large number of approximations made in the calculations, it is concluded that radiative transfer due to the 15 μ bands of carbon dioxide is not significantly different from equilibrium at the mesopause level, for the smoothed atmosphere.

The effect of other temperature gradient discontinuities can be seen at 90 and 60 km. Only one atmospheric layer was used for the stratopause,

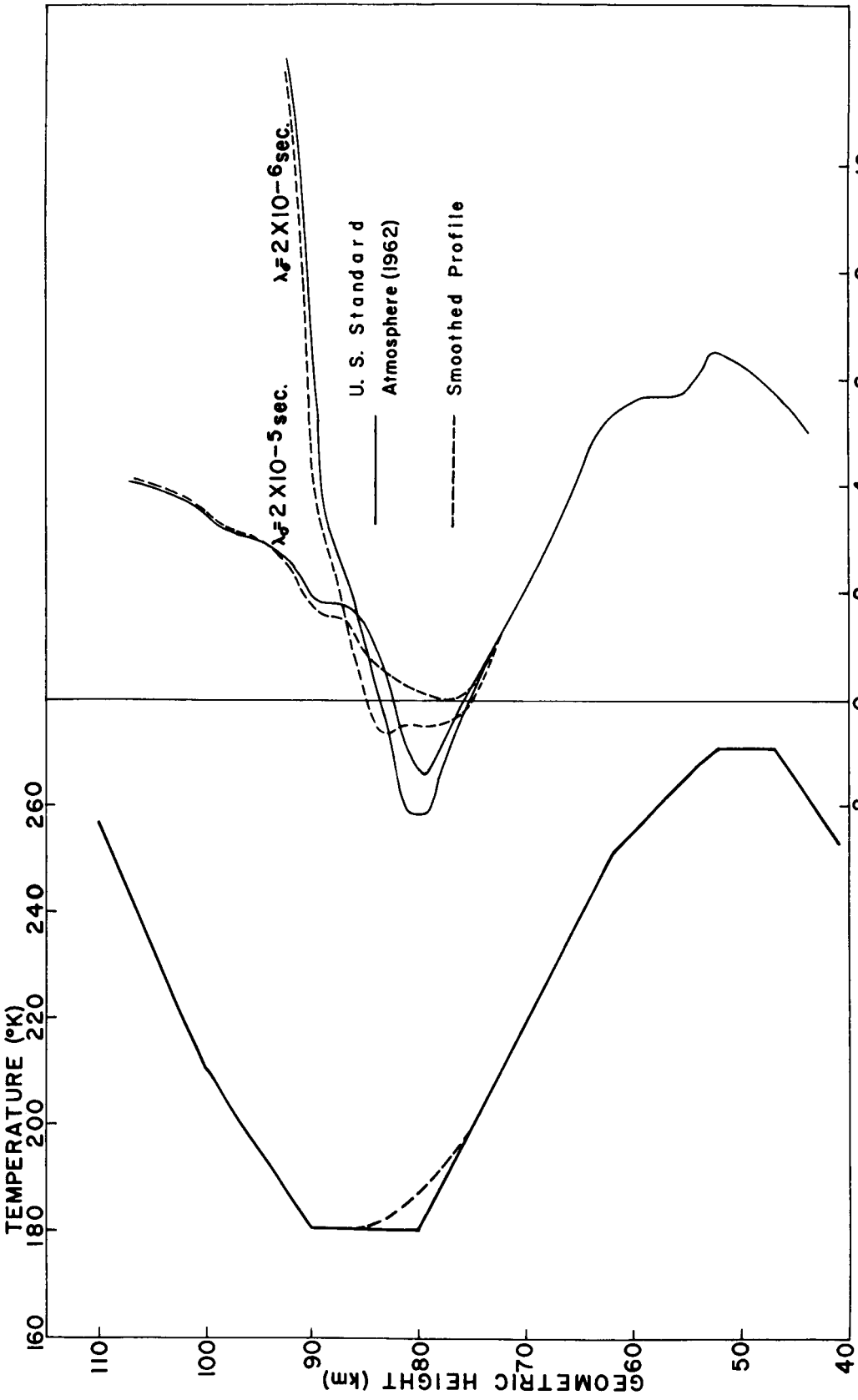

Fig. 4. Calculated cooling rates for modified U.S. Standard Atmosphere (1962).

but if a model of greater resolution is used for this region of the atmosphere, two maxima of cooling obtained, at the bottom and top of the isothermal layer, a result which was also reported by Plass (1956b).

A study of the cooling rates for the individual bands reveals that the weak overtone bands are insensitive to local changes in temperature gradient, and that the same is true of the less abundant isotopes. Only the fundamental of $^{12}C\ ^{16}O_2$ showed a large change from the cooling of the unsmoothed standard atmosphere, although band 1 of isotope 1 and band 4 of isotope 6 also show smaller differences. This result is to be expected since the bands with weak atmospheric absorption are almost transparent over 2 or 4 km layers in the upper atmosphere, and cooling does not depend on the temperature gradient in the neighborhood of the level under consideration.

Calculations have also been made for the ARDC-1959 and the CIRA-1961 model atmospheres. The ARDC-1959 (Minzner et al., 1959) atmosphere has a cold mesopause, typical of average conditions in summer at high latitudes. Similar calculations have been reported by Kondrat'yev et al., (1966) and these are of particular interest since separate results are given for the fundamentals of $^{12}C\ ^{16}O_2$, and the sum of the contributions of the remaining isotopes. Full details of the method of calculation are not given but presumably follow the developments of Shved (1964, 1965a and 1965b), which feature

(a) non-overlapping lines.

(b) allowance for temperature dependence of line intensities.

(c) isothermal layers.

(d) individual relaxation of bands.

(e) line half-widths temperature independent.

Comparison of the cooling rates of this calculation with those of Kondrat'yev et. al., are shown in Fig. 5. The rates for the less abundant isotopes show agreement to within the error that the values can be determined from the figure. For $^{12}C\ ^{16}O_2$ the cooling rates are still quite close, both showing a heating of about 1 deg K/day near 80 km. In the present calculation this heating is localized near the lower mesopause where the temperature gradient is discontinuous. Kondrat'yev et al., shows heating spread over a layer twice as thick. As with Kuhn, the present calculation shows a small but consistantly larger cooling rate throughout the mesosphere. In the lower thermosphere Kondrat'yev et al., have slightly smaller cooling rates.

Unlike the other two models, the CIRA 1961 atmosphere (Kallmann-Bijl et al., 1961) has a smooth profile, with slowly changing temperature gradients. This characteristic is reflected in the sum of the cooling rates due to the fundamentals (all isotopes) (Fig. 6). Depending on the relaxation time λ_o a small amount of either heating or cooling is indicated at the mesopause. In contrast, Kondrat'yev et al., show approximately 0.5 deg/day additional heating at this level, with the heating region again of larger vertical extent.

Although the differences between the present results and those of Kondrat'yev et al., are small, they are consistent. Possible reasons for

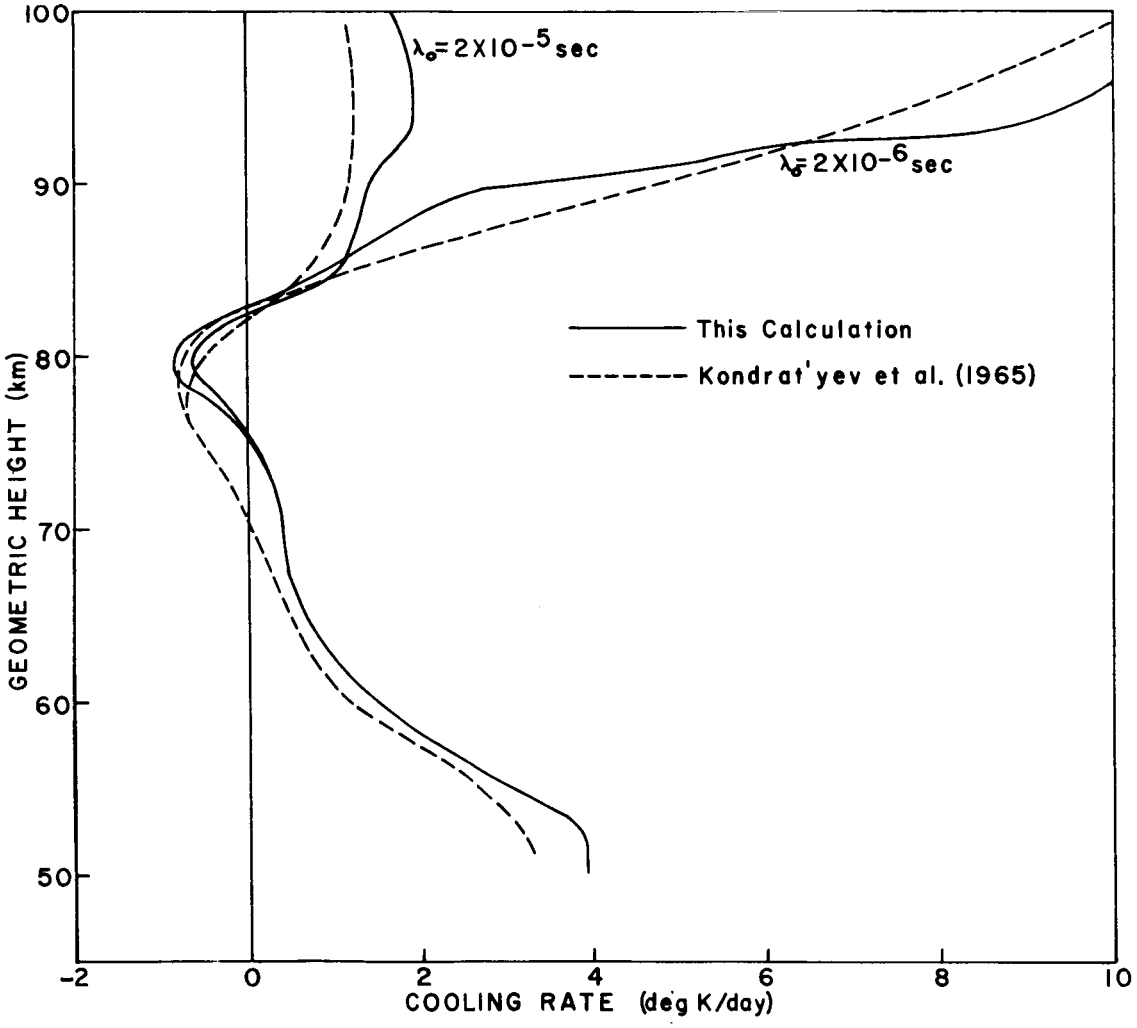

Fig. 5. Calculated cooling rates for ARDC-1959 atmosphere.

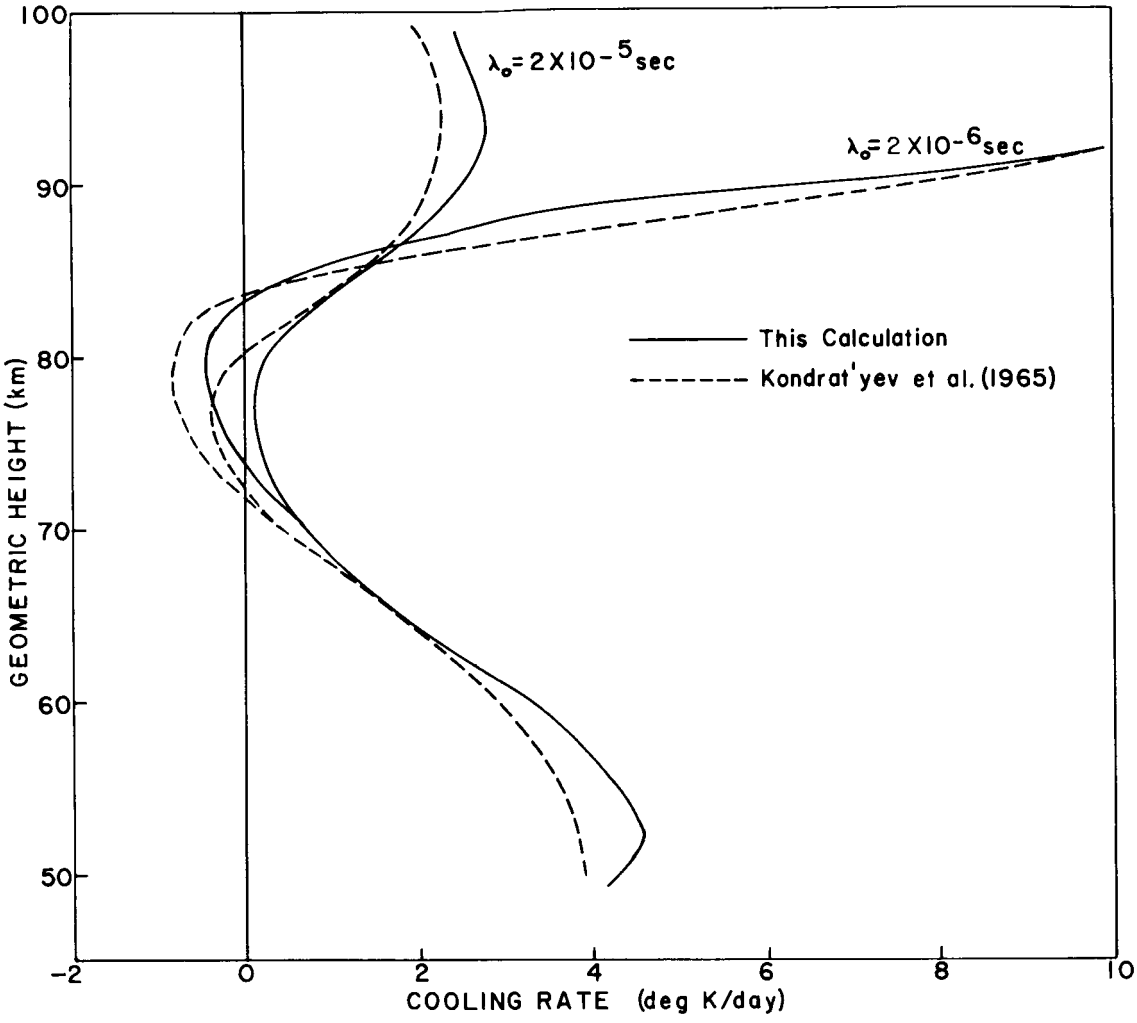

Fig. 6. Calculated cooling rates for CIRA-1961 atmosphere.

these are:

(a) the use of isothermal layers, already discussed.

(b) the use of temperature independent line half-widths: this assumption has been discussed by Hummer and Rybicki (1966), who showed that variations in Doppler half-widths with temperature can be significant in some situations.

3.4.2 Cooling Rates for Measured Temperatures Profiles

Although model atmospheres are of interest as objects of study in their own right, they are nevertheless different from real atmospheres, in that the omnipresent irregularities in the profiles have been removed. The study of the model atmospheres shows that, for the $^{12}C\ ^{16}O_2$ fundamental, local features largely determined the cooling behavior near the mesopause, so that it is natural to expect the fine structure of the atmosphere to be critical in determining cooling rates. Temperature oscillations of up to 30-40°C are not uncommon between 70 and 90 km. (Theon et al., 1967), and these oscillations frequently exhibit a wave-like structure in the vertical.

The profiles used are from Jones and Peterson (1967) and Peterson (1967), measured by the falling sphere technique. Above the maximum altitude of the soundings, the temperature was extrapolated to agree with the U.S. Standard Atmosphere (1962) at 120 km; the structure at these levels is irrelevant to the cooling rate near the mesopause.

Like the calculations for the model atmospheres, a resolution of 2 km

was used between 70 and 90 km, and approximately 5 km layers elsewhere. To reduce computing time the coefficients for the U.S. Standard and Atmosphere (1962) were used to calculate cooling rate for each profile i.e., the temperatue dependence was neglected. The results showed that the fundamental of $^{12}C\ ^{16}O_2$ is by far the most important band, and the temperature dependence for this band is small.

Figure 7 show the temperature structures and calculated cooling rates for six soundings, for the two values of vibrational relaxation time $\lambda_o = 2 \times 10^{-6}$ sec and 2×10^{-5} sec. The contributions from all isotopes and all bands are included.

Before commenting on the individual soundings, some general features common to all the profiles are immediately noticeable.

(a) The smooth features of the cooling rates for model atmospheres are no longer apparent. Instead, large variations in heating and cooling rates are indicated, corresponding to the maxima and minima of the temperature profiles or change in temperature gradient.

(b) There appears to be a marked tendency for greater overall cooling, particularly for the larger value of vibrational relaxation time; for most, but not all, the profiles the heating is restricted to rather thin layers.

(c) In the mesosphere and mesopause region, the maximum cooling rate is frequently about the same or greater than the cooling rate at the much warmer stratopause.

(d) For most profiles the cooling rate is the same for both values

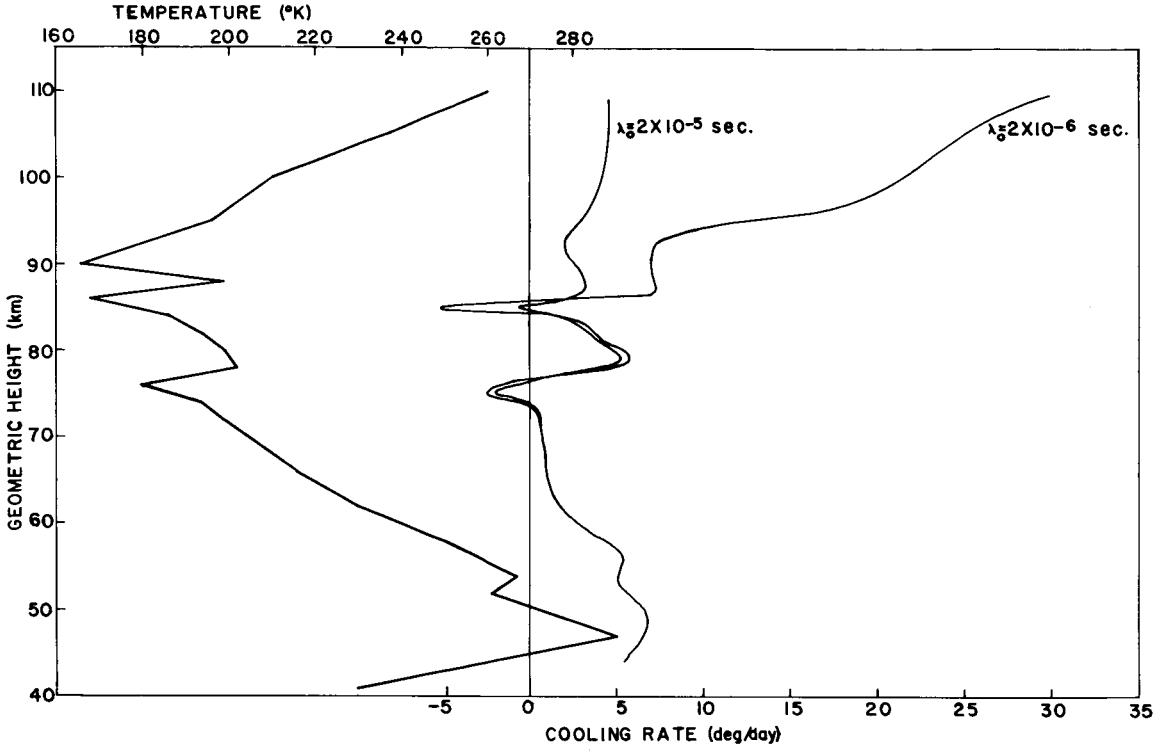

(a) Wallops Island, 38°N, 75°W, 1330 EST, 7 Aug, 1965.

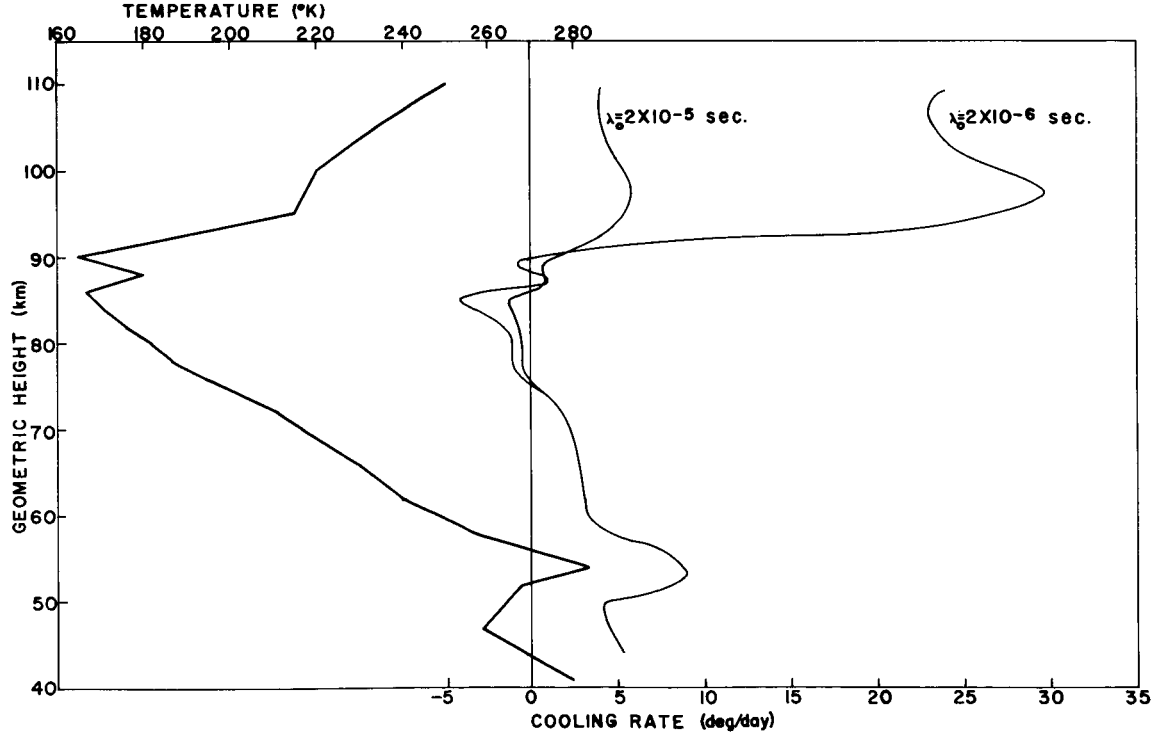

(b) Wallops Island, 38°N, 75°W, 2240 EST, 7 Aug, 1965.

Fig. 7. Calculated cooling rates for measured temperature profiles.

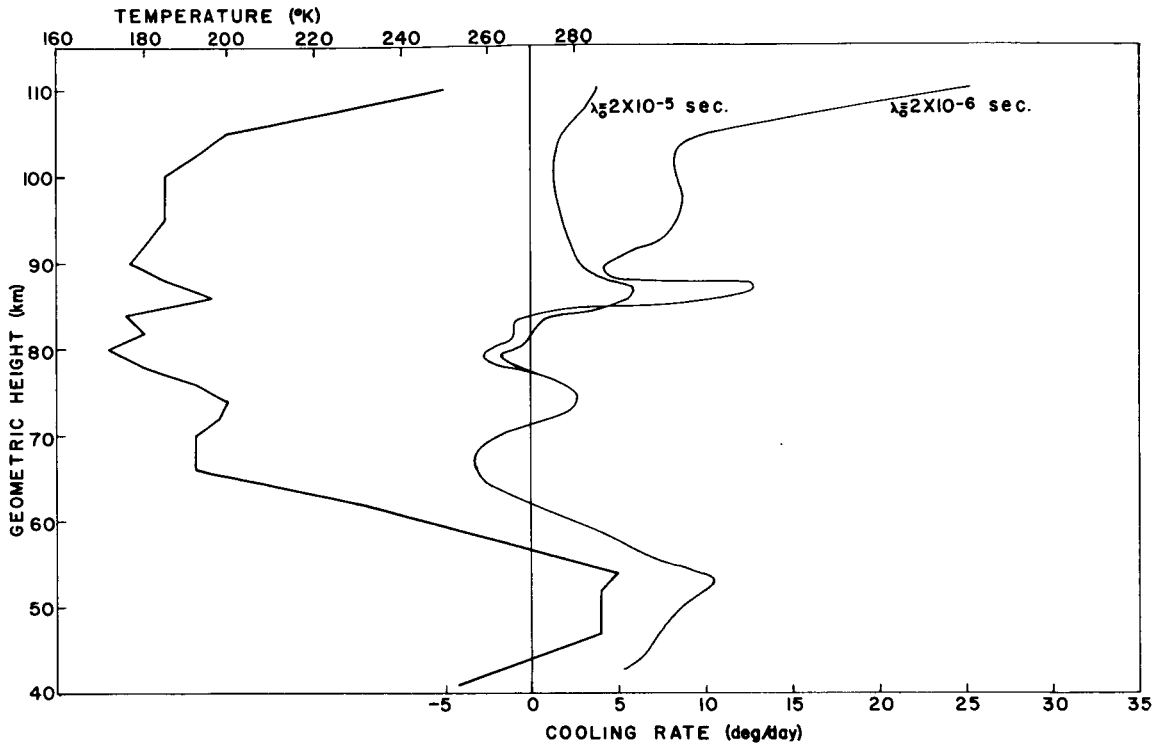

(c) Wallops Island, 38°N, 75°W, 0340 EST, 8 Aug, 1965.

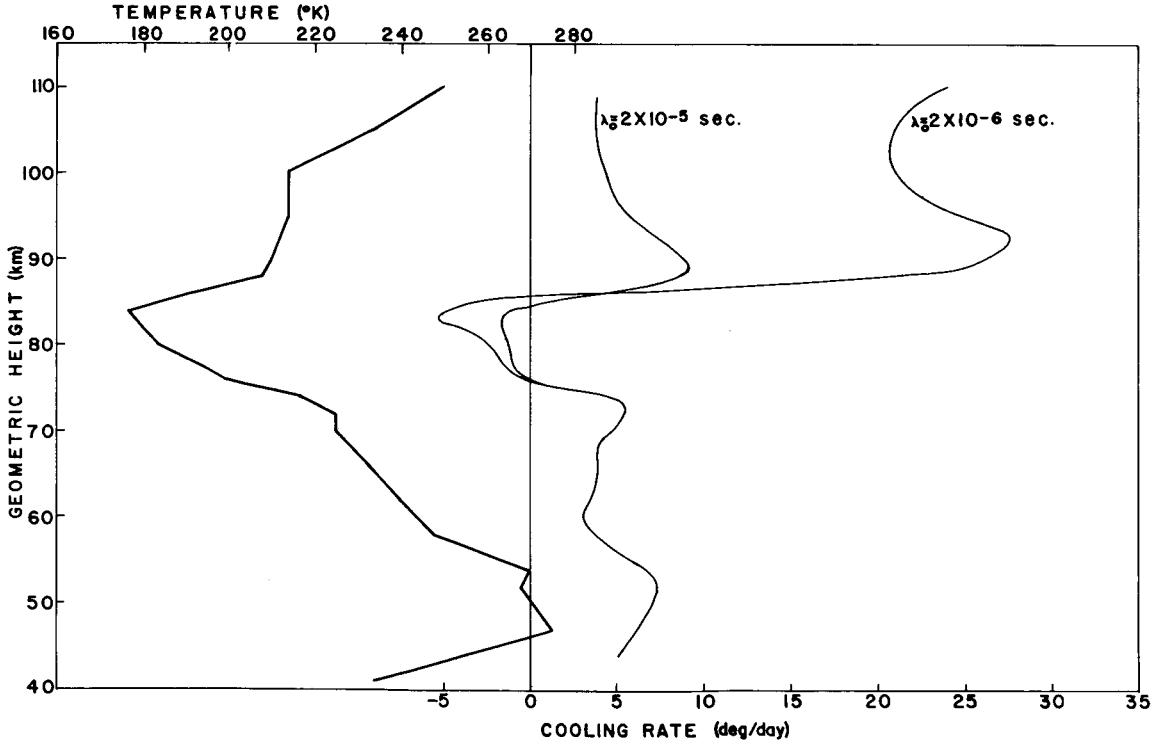

(d) Wallops Island, 38°N, 75°W, 1810 EST, 19 Oct, 1965.

Fig. 7. (Continued)

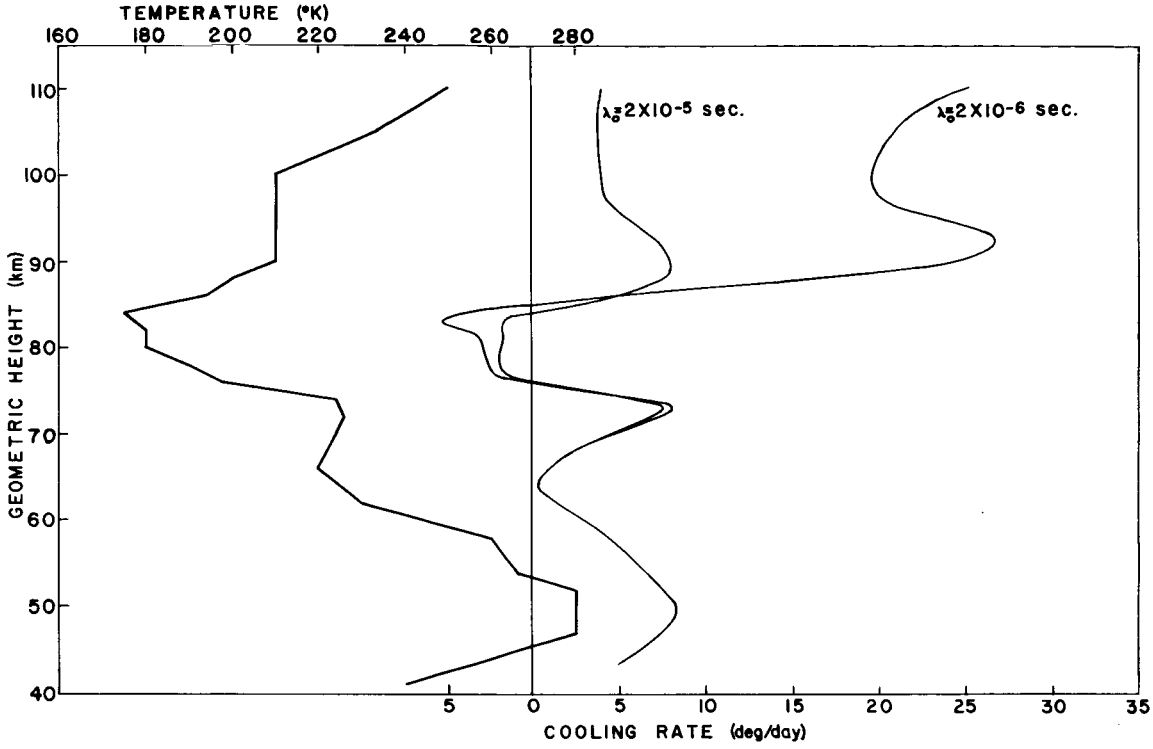

(e) Wallops Island, 38°N, 75°W, 1114 EST, 23 Oct, 1965.

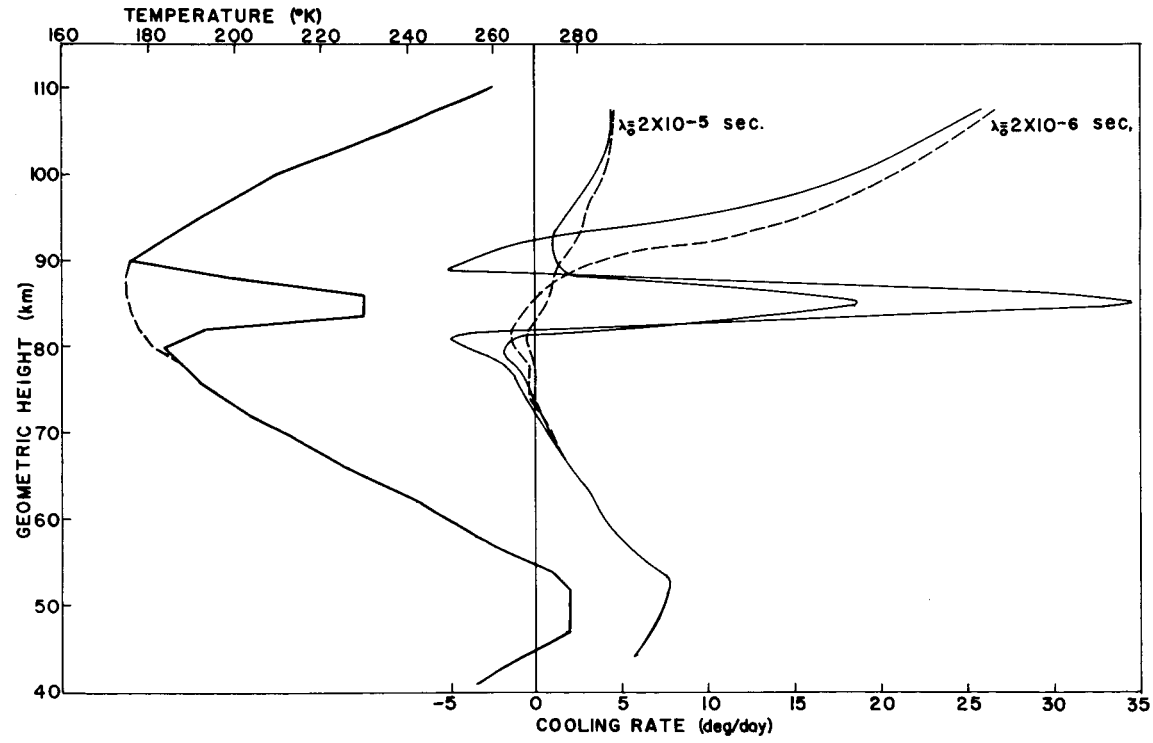

(f) Point Magu, 33°N, 119°W, 14.30 PST, 24 Oct, 1966.

Fig. 7. (Concluded)

of vibrational relaxation time below 75 km, although small differences occur down to 70 km for some of the soundings.

The first three profiles (Figs. 7 (a), (b), and (c)) are from consecutive soundings taken within a 24 hour period in August 1965 at Wallops Island. Each shows some oscillatory temperature structure in the mesopause region. The maximum cooling rate between 90 and 70 km for the first sounding is about 7 deg K/day for $\lambda_o = 2 \times 10^{-6}$ sec. The radiative transfer due to the 15 μ bands of CO_2 is incapable of explaining by itself the reduction by about 20°K of the temperature maximum at 88 km during the 10 hour interval between the first and second soundings. The oscillations increase during the night and are more marked in the third sounding. Although the carbon dioxide plays a substantial role in the transfer of energy at these levels, it is clear that even more important dynamic processes are controlling the temperature profile.

Soundings (d) and (e), taken in October 1965 at Wallops Island, have similar temperature gradient discontinuities in the mesosphere near 70 km which provide large cooling at this level. The mesopause is particularly well defined with the temperature rising rapidly above the temperature minimum. This characteristic explains the substantial heating observed around 80 km for both soundings.

Figure 7 (f) shows a remarkable sounding from Point Magu on 24 October 1966. A temperature perturbation of amplitude almost 50°K was obtained at 85 km. Smaller perturbations are common at this level, but this amplitude is apparently one of the largest recorded. As expected, this perturba-

tion produces a large cooling rate, of about 35 deg K/day for $\lambda_o = 2 \times 10^{-6}$ sec, and 17 deg K/day for $\lambda_o = 2 \times 10^{-5}$ sec. A heating of comparable magnitude might have been expected in the region of temperature minimum immediately above and below the warm layer, but its value is only about one seventh that of the maximum cooling rate. Also shown is the cooling rate obtained in the absence of the temperature perturbation, with near equilibrium conditions at the mesopause.

The calculations for the measured profiles show that the cooling implied by mean atmospheres is not the same as the mean cooling derived from individual soundings. This result is significant for an understanding of the energy balance in the mesopause region of the atmosphere; radiative transfer by carbon dioxide may be able to provide a mean energy sink, particularly for situations in which waves are being propagated vertically.

The effect of temperature oscillations on cooling rates has been discussed by Goody (1964) and by Sasamori and London (1966) for homogeneous atmospheres. In the mesosphere the atmosphere is not homogeneous, or even approximately so, and the departure from local thermodynamic equilibrium makes it impossible to apply their methods.

The calculations made in this section used a vertical resolution of 2 km between 70 and 90 km. The method could be applied to soundings of higher vertical resolution if reliable sounding data become available. The profiles available are not suitable for this application, since they contain a considerable amount of high frequency noise.

3.4.3 Comparison with Previous Calculations

A full comparison of the methods and results of the calculations of Kondrat'yev (1965) and Kuhn (1966) has already been made in the previous sections. Young (1964) attempted calculations that were essentially similar to those of Kuhn, but was unable to obtain cooling rates because of numerical difficulties.

At the time that Curtis and Goody (1956) made their calculations fast computers were not so readily available. They chose an iterative procedure to solve the radiative transfer equations using as an initial guess for the flux divergence the 'cooling to space' (i.e., the amount of energy lost directly to space), a concept that has appeared a number of times in radiative transfer literature. In the mesopause region it has been shown that for strong bands the cooling is dependent on the local temperature structure, while for weak bands heating, rather than cooling, takes place. Lower in the atmosphere where absorption is stronger, the local structure may dominate all but the weakest bands, so that 'cooling to space' cannot be expected to provide a reasonable approximation to the cooling rate. Moreover, iterative procedures for solving the transfer equations have been shown to converge extremely slowly and to depend on the initial guess, and may even diverge (Kuhn, 1966). Curtis and Goody do not make it clear what weak lines, if any, were included or if the less abundant isotopes were considered. These lines have been shown to be important. Murgatroyd and Goody (1958) also made calculations for themesosphere, citing Curtis and Goody for the method of computation. Because of the uncertanties in

the actual parameters and method used, no direct comparison can be made between their results and the present calculations.

The calculations of Prabhakara and Hogan (1966) contain two serious errors. The first lies in the attempt to simulate the absorption in given spectral regions by lines of constant intensity and frequency spacing, using transmission tables of Stull et al., (1963) to deduce some of the parameters. The transmission tables contain the contributions from lines of many different intensities, so that the simple model cannot be expected to represent the transmissivity accurately, especially when extrapolated to low pressures. A further consequence of this treatment is that all bands are considered together, instead of treating the relaxation separately for each band.

The second error lies in the method of solution of the radiative transfer equation. The energy absorbed by a horizontal layer in the atmosphere is

$$2\pi \int_{\nu} \int_{\mu} I(\nu,\mu,\tau)\mu[1-\gamma(\nu,\mu)]\, d\mu\, d\nu$$

where γ is the transmissivity of the layer. This equation is correct. However, Prabhakara and Hogan applied it using the average values of I and γ over finite frequency intervals, i.e., they integrated over frequency assuming that the integral of the product $I(\nu)\ [1-\gamma(\mu)]$ is equal to product of the integrals of $I(\nu)$ and $[1-\gamma(\nu)]$. In fact, $I(\nu)$ is closely correlated with $\gamma(\nu)$. When the absorption is large the radiation originates from a region near the layer under consideration. Conversely, when

the absorption is small, the radiation originates from deep in the atmosphere.

The method used by Prabhakara and Hogan is the finite difference form of Eq.(2.1.6). Their assumption is equivalent to replacing the integral

$$\int_\nu (I_\nu - J_\nu)\, k_\nu \, d\nu \quad \text{by} \quad \int_\nu k_\nu \, d\nu \cdot \int_\nu (I_\nu - J_\nu)\, d\nu$$
$$= S \int_\nu (I_\nu - J_\nu)\, d\nu$$

where S is the total band intensity. This reasoning is false.

The same method was also applied to the Martian atmosphere (Prabhakara and Hogan, 1965).

3.5 SUMMARY AND CONCLUSION

The most important results of the investigation of radiative cooling due to carbon dioxide in the mesosphere and mesopause are:

(a) The equation linking the source function to the flux divergence should contain a degeneracy factor.

(b) Although some radiative heating near the mesopause is typical, its magnitude is small and is usually correlated with either a temperature minimum or an abrupt change in temperature gradient.

(c) Oscillations in the temperature structure near the mesopause dominate the cooling rate, resulting in a considerable increase in cooling at this level. Most of this cooling is provided by the $^{12}C\ ^{16}O_2$ fundamental, with the other bands playing a minor role. When the profile is smooth, the remaining bands (fundamentals of the isotopes and overtone

bands of $^{12}C\ ^{16}O_2$) have a role approximately equal to that of the $^{12}C\ ^{16}O_2$ fundamental.

(d) Vibrational relaxation begins to influence the cooling rate above about 75 km. Uncertainties in the vibrational relaxation time lead to large uncertainties in the cooling rate above this level.

The mesosphere is not in radiative equilibrium (Leovy 1964a and 1964b). This has also been demonstrated by the series of soundings at Wallops Island. However, there can be little doubt that radiative cooling is an important factor in determining the atmospheric temperature profile in the mesosphere and mesopause and that it must be accurately accounted for in any model of this part of the atmosphere. Mean temperature profiles cannot be used to derive mean cooling rates. Wave-like temperature oscillations in the vertical, which are lacking in simple models, are essential in the determination of mean cooling rates.

CHAPTER 4

APPLICATION TO THE ATMOSPHERE OF MARS

4.1 INTRODUCTION

In the last decade significant advances have been made in observations of the surface and atmosphere of Mars. These have come from ground based spectral observations, including the remarkable high resolution interferometric observations of Connes and Connes, 1966, and also from a planetary fly-by mission.

Plans are now being made for the soft-landing of scientific packages on the surface, and for manned exploration at a later date. It would be of significant help to the spacecraft designers to know the range of meteorological conditions such as temperature, pressure, wind velocity to be expected at the surface.

Meteorologists are also interested in the Martian atmosphere. Its structure appears to be simpler than that of the earth's, and therefore interesting for general circulation studies. The virtual absence of clouds and of water vapor from the atmosphere and oceans from the surface is in marked contrast to conditions on the earth. Long wave radiative transfer, in particular that due to carbon dioxide, is of great importance.

The calculations described in this chapter are designed to be used in conjunction with a simple atmospheric circulation model. An essential requirement is that the flux divergence must be simple and quick to evaluate, since it has to be calculated many times.

4.2 ATMOSPHERIC COMPOSITION

It has been known for a number of years that the Martian atmosphere contains considerable amounts of carbon dioxide (e.g., Grandjean and Goody, 1955), deduced from the absorption spectra of reflected solar radiation. Beginning with Kaplan et al., (1964) a series of more precise measurements was made of the carbon dioxide content and the surface pressure. The Mariner IV occulation experiment has also provide valuable information on the surface pressure and composition of the Martian atmosphere (Kilore et al., 1965). Although the exact amount of carbon dioxide is still somewhat uncertain, the amount in a vertical column is believed to be in the range 68 ± 26 m atm., (a partial pressure of 5 ± 2 mb at the surface) and the surface pressure between 5 and 13 mb (Belton and Hunten, 1966). Thus, carbon dioxide is a major atmospheric constituent and the possibility that the atmosphere consists almost entirely of carbon dioxide is not inconsistent with the spectroscopic observations, nor with the occultation observations of Kilore et al.

The amount of water vapor in the atmosphere is small. Kaplan et al., (1964) deduced 14 ± 7 μ precipitable water from their observations but, as in the earth's atmosphere, the amount may be variable. Kaplan et al., also failed to detect any molecular oxygen in the atmosphere, and set an upper limit of 70 cm atm. This implies that the amount of ozone in the atmosphere is strictly limited, and is consistent with the detection of carbon monoxide in Martian spectra, approximately three orders of magnitude

less abundant than carbon dioxide (Kaplan, 1967). Kaplan was also able to deduce that the relative abundance of the isotopes ^{12}C, ^{13}C, ^{16}O, ^{17}O, ^{18}O is approximately the same as in the earth's atmosphere.

Although there are still uncertainties in the exact composition of the Martian atmosphere, the important constituents, particularly those that affect long wave radiative transfer, are known quite well. In any case, a circulation model is probably not sensitive to small uncertainties, and new calculations can easily be undertaken when more accurate data become available. In the radiative transfer calculations described here, a pure CO_2 atmosphere was chosen, with a surface pressure of 6 mb.

The influence of water vapor was neglected; Goody and Belton (1967) have shown its influence to be small. Carbon monoxide has no vibration—rotation band in the thermal infrared region, but a pure rotation band with lines between 100 and 600 μ has been detected. Thus, the radiative role of CO is small and was also neglected.

4.3 CALCULATION DETAILS AND RESULTS

The details of the bands of carbon dioxide in the 15 μ region have already been given in the previous chapter, and the abundance of the isotopes was left unchanged. The only major change is in the Lorentz half-width of the lines, which are now self-broadened. Burch et al., (1962) have shown that the self broadened half-width is about 1.3 times the nitrogen broadened value, i.e., about 0.105 cm^{-1} at 1 atmosphere and 300°K. This is the value used in these calculations. Madden (1961) has

shown that there are variations in half-width with rotational quantum number in the 15 μ region, and these should be taken into account. However, the correct value is not known for all lines, and probably does not have a large effect, especially when compared to other uncertainties in the model. Mixed Doppler-Lorentz broadening was used throughout the Martian atmosphere.

The atmospheric model used for the circulation calculations is quite simple. The atmospheric temperature profile is defined by the temperature at three presure levels. $p_g/3$, $2p_g/3$ and p_g, where p_g is the surface pressure. At pressures lower than $p_g/3$ the atmosphere is isothermal. At higher pressures the temperature is given by a quadratic in logarithm of pressure, through the three pressure levels.

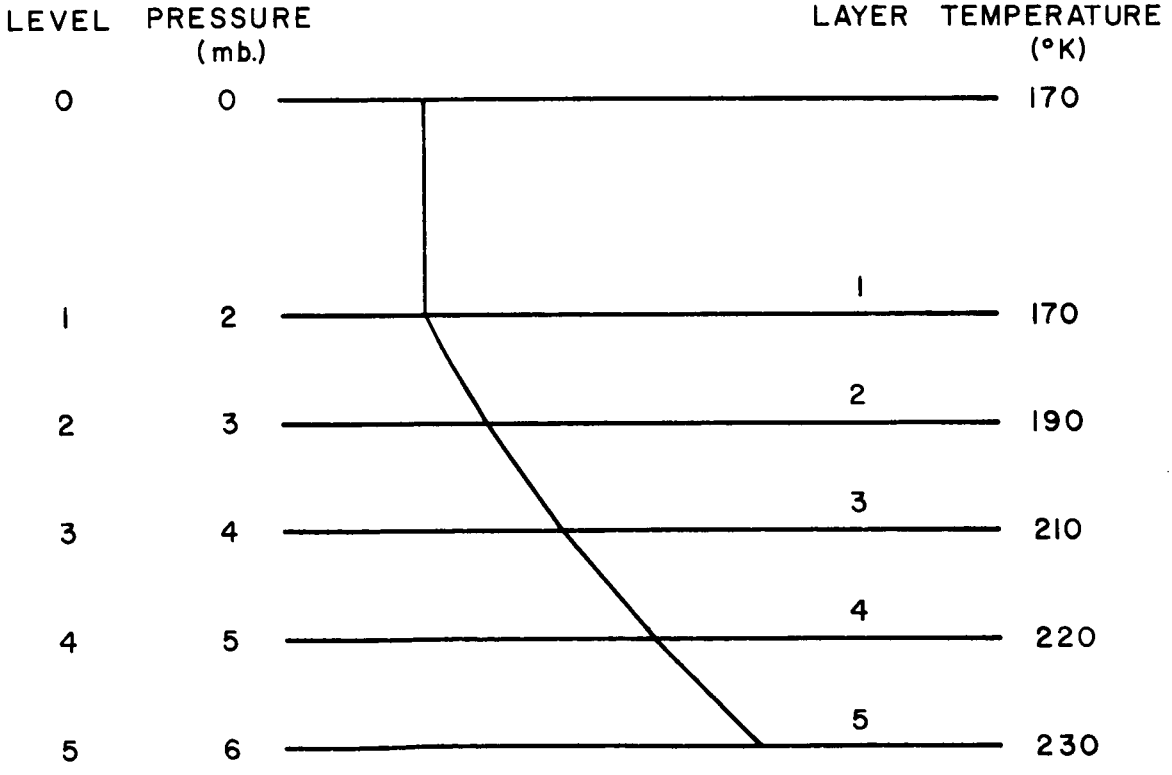

Fig. 8. Model of Martian atmosphere, showing temperatures and pressures used in radiative transfer calculations.

For the radiative transfer calculation, two further levels at $p_g/2$ and $5p_g/6$ were inserted, and the calculation methods described in Chapter 2 were applied to this simple atmosphere.

From Eq. (2.4.7), the flux difference between adjacent levels may be written in the form

$$\Delta F_m = \sum_{\nu} \sum_{i=1}^{5} a_{mi} J_i \qquad m = 1,\ldots,5 \tag{4.3.1}$$

In order to arrive at this form of the equation the source function (identical to the Planck function in these calculations) has to be assumed frequency independent over finite frequency intervals. It was found that using the average value of J_i in 10 cm^{-1} intervals was satisfactory. This should be contrasted to the mesospheric calculations in Chapter 3, where the source function was assumed constant over a whole absorption band, approximately 100 cm^{-1} wide.

In each of the 10 cm^{-1} intervals the source function J_i was expanded in the form

$$J_i(\bar{\nu},T) \sim d_{o,i} + d_{1,i}\, T + d_{2,i} T^2 \tag{4.3.2}$$

The coefficients $d_{o,i}$, $d_{1,i}$ and $d_{2,i}$ were obtained by requiring the quadratic expression to be exact for three temperatures, T_i and $T_i \pm 30°K$. In this way an error of less than 1% can be obtained over the range $T_i \pm 50°K$. The T_i's used are given in Fig. 8.

Substituting Eq. (4.3.2) into Eq. (4.3.1), ΔF_m may be expressed in the form

$$\Delta F_m = a_m + \sum_{i=1}^{5} (b_{m,i} T_i + C_{m,i} T_i^2) \quad m = 1,2,\ldots,5 \tag{4.3.3}$$

One difficulty remains: the coefficients a_{mi} in Eq. (4.3.1) are functions of temperature, because of the dependence of line intensity and half-widths on temperature, and should therefore only be used for the temperature profile for which they are calculated. The temperature dependence of a_{mi} could be allowed for in a simple way by expanding the coefficient as a linear function of $T_1,\ldots,T_5$, but the amount of computation involved would be very large since the integration over the whole band would have to be made for many temperature profiles.

In view of the many assumptions made in the atmospheric circulation model, the temperature dependence of the coefficients was neglected. In theory, the dependence is easy to account for but practical limitations on computing time make it impossible at the present time.

The values of the coefficients are shown in Table V. The accuracy of solution using Eq. (4.3.3) was compared with that of Eq. (4.3.1) for an extreme profile, assuming the atmosphere to be 50°K colder than the mean profile at all levels. The largest error was about 0.5 deg K/day in the cooling rate. These results are shown by way of example. It is clearly possible to repeat the computations as necessary, for any desired model atmosphere.

Table VI shows the cooling rates derived from several representative temperature profiles.

TABLE V

HEATING RATE COEFFICIENTS FOR THE MARTIAN ATMOSPHERE

A(1)	-.31658E+02				
B(1,1)...B(1,5)	.65578E+00	-.96416E-01	-.22109E-01	-.90128E-02	-.16149E-01
C(1,1)...C(1,5)	-.26919E-02	.37790E-03	.84839E-04	.34486E-04	.61785E-04
A(2)	-.11207E+02				
B(2,1)...B(2,5)	.20483E+00	.26009E+00	-.19079E+00	-.36926E-01	-.49174E-01
C(2,1)...C(2,5)	-.84228E-03	-.10202E-02	.73195E-03	.14135E-03	.18819E-03
A(3)	-.19648E+02				
B(3,1)...B(3,5)	-.22993E+00	.51254E+00	.33239E+00	-.22086E+00	-.11244E+00
C(3,1)...C(3,5)	.94419E-03	-.20080E-02	-.12735E-02	.84507E-03	.43014E-03
A(4)	-.19465E+02				
B(4,1)...B(4,5)	-.45554E-01	-.23934E+00	.54998E+00	.38205E+00	-.37851E+00
C(4,1)...C(4,5)	.18731E-03	.93777E-03	-.21044E-02	-.14587E-02	.14504E-02
A(5)	-.14975E+02				
B(5,1)...B(5,5)	-.23383E-01	-.42701E-01	-.26976E+00	.54628E+00	.00000E+00
C(5,1)...C(5,5)	.96087E-04	.16736E-03	.10332E-02	-.20834E-02	.00000E+00

TABLE VI

HEATING RATES IN THE MARTIAN ATMOSPHERE FOR TYPICAL TEMPERATURE PROFILES

	Temperature at level I (°K) or heating rate in layer I (°K/Day)				
I	1	2	3	4	5
Temperature	170	190	210	220	230
Heating	-4.3	1.4	-3.7	-7.6	-10.0
Temperature	170	190	210	220	250
Heating	-4.0	2.3	-1.8	-1.3	-10.0
Temperature	170	190	210	220	210
Heating	-4.5	0.8	-5.3	-12.8	-10.0
Temperature	170	190	210	210	200
Heating	-4.7	0.2	-7.3	-12.5	-6.5
Temperature	190	210	230	240	250
Heating	-8.8	0.5	-6.7	-11.4	-13.8
Temperature	170	180	190	210	230
Heating	-5.0	-0.3	0.7	-0.4	-9.6

The form of the solution in Eq. (4.3.3) is simple and quick to evaluate, and therefore meets the requirements for use in the circulation model.

4.4 COMPARISON WITH PREVIOUS CALCULATIONS

Calculations of radiative transfer in the Martian atmosphere have been made by Ohring and Marino (1966) for several different combinations of surface pressure and atmospheric composition, although not for pressures as low as 6 mb. Their long-wave radiative transfer considered only the 15 μ bands of carbon dioxide, using a modified form of Elsasser's (1960) radiation tables. It is not clear exactly what allowance was

made for temperature effects. Their results showed stratospheric equilibrium temperatures some 15 to 20°K lower than those of Prabhakara and Hogan (1965). This may be a consequence of the error in computing the absorbed radiation in the latter paper, as discussed in section 3.4.3.

The results of Ohring and Marino cannot be directly applied to a circulation model, although they could probably be modified to do so. However, calculations by Leovy (Leovy, 1966 and Leovy and Mintz, 1966) were made specifically for this purpose. The transmissivities were calculated by the same method as Prabhakara and Hogan (1965), which introduces an unknown error. However, the manner of calculating transmissivities is not essential to the method. The circulation model used by Leovy and Mintz assumes a constant lapse rate in the troposphere (except for a surface boundary layer), making the temperature dependence of the transmission functions easier to incorporate. A similar method could probably be used for the calculations described here, although it may be better to use the constant coefficients initially to test the circulation model, and to modify them afterwards when it becomes apparent precisely what kind of temperature variations can be expected.

CHAPTER 5

CONCLUSIONS

The main result of this study is the development of a method of computing flux divergences in a plane parallel atmosphere by direct integration with respect to frequency over molecular absorption bands. Direct integration methods, which have already been used to calculate atmospheric slant path transmissivities, offer advantages over previous methods:

1. The Curtis-Godson approximation is applied over successive thin atmospheric layers, instead of thick layers.

2. Band models are completely avoided and the actual position, intensities and half-widths of the lines are used, at least to within the accuracy that they are known.

The calculation of flux divergences by direct integration shares these two advantages, but also makes possible other features:

3. A diffusivity factor is not employed. Instead, exponential integrals are used and efficient polynomial approximations for $E_2(x)$, $E_3(x)$ and $E_3(x)$ have been developed.

4. A source function which is linear in pressure in thin horizontal layers is used. It is shown to be more accurate than using isothermal layers or higher order polynomials to approximate the source function.

5. Flux differences rather than fluxes are calculated, avoiding numerical difficulties when the differences are small. This is important at low pressures where small differences in flux can provide large amounts

of cooling. The atmospheric layers can be made arbitarily thin to accomodate fine structure in the vertical temperature profile.

6. The method is versatile and can be used for any absorber or mixture of absorbing gases.

The disadvantages of the method are:

1. It requires an intimate knowledge of atmospheric absorption bands, although this is true to a large extent of any method.

2. It requires comparatively large amounts of computing time. This factor can be expected to decrease in the future as faster electronic computers are developed, and computing becomes less expensive.

Two applications of the method are given. The first is to the earth's atmosphere between about 60 and 100 km, where radiative cooling due to the 15 μ carbon dioxide bands is investigated. Vibrational relaxation is taken into account to derive source functions for the individual bands. Cooling rates are obtained for both model atmospheres and actual soundings. The results show that cooling predominates near the mesopause, but that slight heating frequently occurs at the temperature minimum or where discontinuities in the temperature gradient exist. Local features of the vertical temperature structure dominate the cooling rate. Vibrational relaxation influences the cooling rate above 70 to 75 km where the rates are strongly dependent on the vibrational relaxation time. The radiative cooling rates calculated from mean profiles are significantly smaller than the mean of cooling rates obtained from measured temperature soundings,

suggesting a possible mean energy sink for the upper mesosphere and lower thermosphere.

The second application is to the Martian atmosphere, where radiative transfer calculations are performed for incorporation in a simple circulation model. A pure carbon dioxide atmosphere and a surface pressure of 6 mb are used to illustrate the method.

CHAPTER 6

SUGGESTIONS FOR FUTURE WORK

The techniques developed in this paper can be applied to a wide variety of atmospheric radiative problems. The speed of the available computer was a definite limitation on the scope of applications described here, but future computing developments will make more extensive computations possible.

The lack of detailed knowledge of the absorption bands of water vapor (6.3 μ and pure rotational bands) and of ozone (9.6 μ bands) prevents the accurate calculation of cooling rates in other spectral regions for the earth's atmosphere. Both experimental and theoretical investigations of these absorption bands are being made and positive results can be expected within a few years. This will make possible the application of the present method to other spectral regions, as well as to the rest of the atmosphere.

In the region of the earth's atmosphere where vibrational relaxation is important, accurate values of relaxation time are needed. An equation for the source function for the carbon dioxide overtone bands in the 15 μ region is required. Because of the influence of local temperature structure features, more calculations using measured profiles are required to determine mean cooling rates near the mesopause, and to obtain an understanding of the role of the 15 μCO_2 bands in the energy balance of the upper atmosphere.

As more details of the composition of the Martian atmosphere become available, it will be possible to modify radiative transfer calculations. The problem of vibrational relaxation in the upper atmosphere is also of considerable interest, but cooling rates may again be dominated by local temperature features, which are unknown at the present time. It would be of interest to apply the present method of calculation to obtain radiative equilibrium temperature profiles.

Although the methods described in this study were developed specifically to examine long-wave radiative transfer, they can be modified and applied to the absorption of solar radiation in the near infrared. An understanding of the combined effect of all radiative transfer processes in the upper atmosphere would constitute a significant advance in atmospheric physics.

APPENDIX

THE POLYNOMIAL APPROXIMATION OF EXPONENTIAL INTEGRALS

In radiative transfer problems angular integration of the transfer equations frequently produces terms involving exponential integrals. The n^{th} order exponential integral $E_n(x)$ is defined by

$$E_n(x) = \int_1^\infty e^{-xt}/t^n \, dt$$

$E_1(x)$ may be evaluated in a number of ways, including series and asymptotic expansions, or less precisely using polynomial or rational approximations. (Abramowitz and Stegun 1964). A recurrence relation may be used to obtain higher order integrals from $E_1(x)$.

The rational approximations are quite suitable for use in a computer subroutine, but they involve the evaluation of the exponential function or natural logarithm, or both (depending on the value of x), a factor which considerably increases computing time. Furthermore $E_1(x)$ has a singularity at the origin, whereas the higher order integrals are well behaved. In addition, values obtained by the recurrence relation for $x > 5$ are subject to considerable error. Thus there are advantages in computing the higher order integrals directly, rather than from the first order integral.

The approach adopted was to approximate the integrals by polynomials of intervals on the positive x-axis, using a least squares technique.

Suppose a polynomial of degree m

$$p_m(x) = \sum_{i=0}^{m} a_i x^i$$

is used in the interval (x_1,x_2). The condition to be satisfied is that

$$\int_{x_1}^{x_2} [p_m(x) - E_n(x)]^2 \, dx$$

is a minimum.

In practice, $p_m(x)$ is expressed in terms of Legendre polynomials $P_i(x)$ which are orthogonal on (x_1,x_2)

$$p_m(x) = \sum_{i=0}^{m} A_i P_i(x)$$

The condition then becomes

$$\int_{x_1}^{x_2} P_i(x)[p_m(x) - E_n(x)] \, dx = 0 \quad i = 0,\ldots,m$$

or

$$A_i C_i = \int_{x_1}^{x_2} P_i(x) E_n(x) \, dx \quad i = 0,\ldots,m \qquad (A\text{-}1)$$

where

$$C_i = \int_{x_1}^{x_2} (P_i(x))^2 \, dx$$

The integral in Eq. A-1 can be expressed as a linear sum of integrals of the form

$$d_j = \int_{x_1}^{x_2} x^j E_n(x) \, dx \quad j = 0,\ldots,i$$

By successive integration by parts, or by induction on j, it can be shown that

$$d_j = \sum_{k=0}^{j} \frac{(j)!}{(j-k)!} [x_1{}^{j-k} E_{n+1+k}(x_1) - x_i{}^{j-k} E_{n+1+k}(x_2)]$$

This method can be used for values of x_1 greater than about 1.0. The values of $E_1(x_1)$ and $E_1(x_2)$ were obtained from published tables and the recurrence relation employed for the higher order integrals. Double precision arithmetic was used.

For small values of x_1 and x_2 the numerical value of the individual terms in the series expansion are many orders of magnitude greater than the sum, so that even double precision does not produce sufficient accuracy. The integrals were evaluated for x_1 and x_2 between 0.0 and 1. 0 by Gaussian quadrature. The values of the exponential integrals at the quadrature points were accurately obtained from the series expansion of $E_1(x)$ (which converges rapidly on this interval), followed by the recurrence relation.

Radiative transfer applications generally require a high absolute accuracy for the exponential integrals, rather than a high relative accuracy. This implies that for larger values of x, the number of significant figures of accuracy may be quite low. The aim of investigation was to produce an efficient method to calculate the exponential integrals to an absolute accuracy of about 1×10^{-7}. For $E_4(x)$ this can be readily achieved, although it requires the interval $(0,\infty)$ to be broken into rather a large number of subintervals. Details are given in Table VII. $E_3(x)$

requires slightly more subintervals but is otherwise similar. Table VIII lists the intervals and coefficients.

Near $x = 0$ $E_2(x)$ presents some problems, since its slope is not finite at $x = 0$, a characteristic which make approximation by a polynomial in this region very difficult. In the interval (0,0.005). function was expanded:

$$E_2(x) \sim 1 + [\gamma - 1 + \ell n\, x]\, x - \frac{1}{2} x^2 + \frac{1}{12} x^3$$

where

γ is Euler's constant.

For $x \geq .005$ a polynomial expansion was employed (see Table IX).

The resulting computer subroutines, although not mathematically elegant, provide a rapid means of evaluating E_2, E_3 and E_4. With the exception of the region near $x = 0$ for E_2, the average time for evaluation is about 0.24 m sec for the IBM 7090, which is almost twice the average speed of the system subroutine for the exponential function.

TABLE VII

COEFFICIENTS FOR THE POLYNOMIAL APPROXIMATION OF $E_4(x)$

X1	X2	N	A(0)	A(1)	A(2)	A(3)	A(4)	A(5)	A(6)
.00	.02	3	.33333321E+00	-.49991784E+00	.48723621E+00	-.40065675E+00			
.02	.10	4	.33333145E+00	-.49976349E+00	.48623636E+00	-.54877654E+00	.67427701E+00		
.10	.20	4	.33329039E+00	-.49820931E+00	.46314345E+00	-.38876234E+00	.23942219E+00		
.20	.40	4	.33300485E+00	-.49306872E+00	.42766140E+00	-.27717782E+00	.10435406E+00		
.40	.70	5	.33253226E+00	-.48847193E+00	.41209314E+00	-.26007762E+00	.11597315E+00	-.26091905E-01	
.70	1.00	4	.32618509E+00	- 44764367E+00	.30568652E+00	-.11924852E+00	.21083163E-01		
1.00	1.50	5	.32369356E+00	-.44028710E+00	.30183790E+00	-.12713362E+00	.31436526E-01	-.34847974E-02	
1.50	2.50	6	.31416286E+00	-.40980641E+00	.26366584E+00	-.10465057E+00	.26191553E-01	-.38024567E-02	.24418347E-03
2.50	4.00	6	.26476052E+00	-.29454781E+00	.14995841E+00	-.43917471E-01	.76716851E-02	-.74718008E-03	.31347324E-04
4.00	6.00	6	.16347779E+00	-.14351490E+00	.54917252E-01	-.11618356E-01	.14224296E-02	-.94971422E-04	.26886468E-05
6.00	8.00	5	.45805090E-01	-.27338178E-01	.66609363E-02	-.82506626E-03	.51796823E-04	-.13152097E-05	
8.00	10.00	4	.61485633E-02	-.24149872E-02	.35942825E-03	-.23983739E-04	.60455421E-06		
10.00	12.00	3	.43135189E-03	-.10716388E-03	.89272471E-05	-.24915099E-06			
12.00	14.00	2	.16129888E-04	-.23012068E-05	.82365827E-07				

TABLE VIII

COEFFICIENTS FOR THE POLYNOMIAL APPROXIMATIONS OF $E_3(x)$

X1	X2	N	A(0)	A(1)	A(2)	A(3)	A(4)	A(5)	A(6)
.00	.01	5	.50000000E+00	-.99927661E+00	.35030680E+01	-.14451565E+03	.91145339E+04	-.27510454E+06	
.01	.05	5	.49998486E+00	-.99367759E+00	.24543231E+01	-.18666429E+02	.16957034E+03	-.78233485E+C3	
.05	.10	5	.49987973E+00	-.98250148E+00	.19531425E+01	-.68473836E+01	.24141827E+C2	-.43633200E+C2	
.10	.20	5	.49950246E+00	-.96447504E+00	.16000413E+01	-.33014884E+01	.59086080E+01	-.53301442E+01	
.20	.40	5	.49797289E+00	-.92834808E+00	.12496552E+01	-.15556700E+01	.14440030E+C1	-.65387457E+C0	
.40	.70	5	.49291603E+00	-.86641115E+00	.93952389E+00	-.76213922E+00	.40763092E+C0	-.10229208E+C0	
.70	1.00	5	.48203747E+00	-.78785009E+00	.70970913E+00	-.42183647E+00	.15271436E+C0	-.25C82541E-C1	
1.00	1.50	5	.46228186E+00	-.69286540E+00	.52553268E+00	-.24177842E+00	.63959788E-C1	-.74386331E-C2	
1.50	2.50	6	.43684018E+00	-.61053170E+00	.42011457E+00	-.17665828E+00	.46264005E-C1	-.69480434E-02	.45746718E-03
2.50	4.00	6	.34656643E+00	-.39789156E+00	.20831318E+00	-.62459659E-01	.11121848E-01	-.10999885E-C2	.46719667E-04
4.00	6.00	6	.20000240E+00	-.17767995E+00	.68695208E-01	-.14662192E-01	.18086938E-C2	-.12154629E-C3	.34603193E-05
6.00	8.00	5	.52636089E-01	-.31518925E-01	.77010713E-02	-.95616821E-03	.60148400E-04	-.15299014E-C5	
8.00	10.00	4	.68132871E-02	-.26793015E-02	.39918259E-03	-.26660540E-04	.67255760E-06		
10.00	12.00	3	.46744948E-03	-.11619393E-03	.96840454E-05	-.27038491E-06			
12.00	14.00	2	.17225127E-04	-.24581282E-05	.88003757E-07				

TABLE IX

COEFFICIENTS FOR THE POLYNOMIAL APPROXIMATION OF $E_2(x)$

X1	X2	N	A(0)	A(1)	A(2)	A(3)	A(4)	A(5)	A(6)
.005	.01	5	.99863854E+00	-.64849862E+01	.28699864E+03	-.20230211E+05	.92987275E+06	-.18864517E+08	
.01	.02	5	.99719845E+00	-.57667626E+01	.14015630E+03	-.48733755E+04	.11095948E+06	-.11211459E+07	
.02	.03	5	.99512047E+00	-.52178244E+01	.81215706E+02	-.16637561E+04	.22506892E+05	-.13650376E+06	
.03	.05	5	.99227478E+00	-.47562499E+01	.50897054E+02	-.65548040E+03	.55339225E+04	-.20871535E+05	
.05	.08	5	.98743435E+00	-.42707709E+01	.31161615E+02	-.24918857E+03	.13013803E+04	-.30413637E+04	
.08	.14	5	.97890829E+00	-.37515615E+01	.18314077E+02	-.87710226E+02	.27097516E+03	-.37351891E+03	
.14	.25	6	.96617789E+00	-.32935617E+01	.11633582E+02	-.38542755E+02	.90594739E+02	-.12506467E+03	.75047464E+02
.25	.40	6	.94232903E+00	-.27602169E+01	.66185588E+01	-.13205705E+02	.18236745E+02	-.14695374E+02	.51126570E+01
.40	.70	6	.91002540E+00	-.23189262E+01	.40972991E+01	-.55123669E+01	.50584481E+01	-.27377738E+01	.65312535E+00
.70	1.00	5	.83257151E+00	-.16824257E+01	.18822436E+01	-.13316793E+01	.54534096E+00	-.97555565E-01	
1.00	1.50	6	.78964619E+00	-.14714204E+01	.14733368E+01	-.95133859E+00	.39167846E+00	-.92110982E-01	.97C39862E-02
1.50	2.50	6	.67680797E+00	-.10419146E+01	.78456730E+00	-.35571203E+00	.98812997E-01	-.15521811E-01	.10573839E-02
2.50	4.00	6	.48261635E+00	-.57616474E+00	.31201874E+00	-.96201227E-01	.17518586E-01	-.17638563E-02	.75988859E-04
4.00	6.00	6	.25318620E+00	-.22816343E+00	.89305974E-01	-.19262687E-01	.23975807E-02	-.16236047E-03	.46529556E-05
6.00	8.00	5	.61520229E-01	-.36981421E-01	.90654130E-02	-.11287050E-02	.71170586E-04	-.18139326E-05	
8.00	10.00	4	.76228002E-02	-.30017878E-02	.44776459E-03	-.29936337E-04	.75588066E-06		
10.00	12.00	3	.50963609E-03	-.12675641E-03	.10569960E-04	-.29525857E-06			
12.00	14.00	2	.18470210E-04	-.26366002E-05	.94418581E-07				

BIBLIOGRAPHY

Abramowitz, M., and I. A. Stegun, 1964: Handbook of Mathematical Functions. NBS Applied Math. Series, 55, 1046 pp.

Belton, M.J.S., and D. M. Hunten, 1966: The abundance and temperature of CO_2 in the Martian atmosphere. Astrophys. J. 145, 454-467.

Benedict, W. S., and L. D. Kaplan: Line parameters for the pure rotational band of water vapor. (Unpublished).

Bolin, B., and C. D. Keeling, 1963: Large-scale atmospheric mixing as deduced from the seasonal and meridianal variations of carbon dioxide. J. Geophy. Res., 68, 3899-3920.

Burch, D. E., D. A. Gryvnak and D. Williams, 1962: Infrared absorption by carbon dioxide, water vapor and minor atmospheric constituents. GRD Research Report, AFCRL-62-698, Air Force Cambridge Res. Labs.

Burch, D. E., D. A. Gryvnak and R. R. Patty, 1965: Experimental Investigation of the absorption of Infrared Radiation. Aeronutronics Technical Report U-3192.

Chandrasekhar, S., 1960: Radiative Transfer. Dover, New York, 393 pp.

Chaney, L. W., S. R. Drayson and C. Young, 1967: Fourier Transform Spectrometer—Radiative measurements and temperature inversion, Applied Optics 6, 347-349.

Clough, S. A., and F. X. Kneizys, 1965: Ozone Absorption in the 9.0 Micron region. Air Force Cambridge Research Laboratories, Phys. Sci. Research Papers NO. 170, 77 pp.

Connes, J. and P. Connes, 1966: Near-Infrared Planetary Spectra by Fourier Transform Spectroscopy. J. Opt. Soc. Am. 56, 896-910.

Curtis, A. R., 1952: Discussion of Goody's, "A Statistical model for water vapor absorption." Q.J.R.M.S., 78, 638-640.

Curtis, A. R., 1956: The computation of radiative heating rates in the atmosphere. Proc. Roy. Soc., 236A, 148-156.

Curtis, A. R. and R. M. Goody, 1956: Thermal Radiation in the Upper Atmosphere. Proc. Roy. Soc. 236A, 193-206.

Drayson, S. R., 1964. Atmospheric slant path transmission in the 15 μ CO_2 Band. University of Michigan, College of Engineering Technical Report 05863-6-T.

Drayson, S. R., 1966: Atmospheric transmission in the CO_2 bands between 12 μ and 18 μ. Applied Optics 5, 385-391

Drayson, S. R. and C. Young, 1966: Theoretical investigations of carbon dioxide radiative transfer. Univ. Michigan, Dept. Aerospace Eng., Final Report 07349-1-F, 56 pp.

Drayson, S. R., S. Y. Li and C. Young, 1967: Final report on project 08183, Dept. Aerospace Eng., Univ Michigan: In preparation.

Elsasser, W. M., 1938: Mean Absorption and Equivalent Absorption Coefficient of a Band Spectrum. Physical Review, 34, 126-129.

Elsasser, W. M., 1942: Heat Transfer by Infrared Radiation in the Atmosphere. Harvard Meteor. Studies, No. 6., Cambridge, Harvard Univ. Press, 107 pp.

Elsasser, W. M., 1960: Atmospheric radiation tables. Meteor. Monogr., 4, No. 23, Boston, Amer. Meteor. Soc, 43 pp.

Gates, D. M., R. F. Calfee and D. W. Hansen, 1963: Computed transmission spectra for 2.7-micron H_2O band. App. Optics, 2, 1117-1122.

Godson, W. L., 1953: The evaluation of infrared radiative fluxes due to atmospheric water vapor. Q.J.R.M.S., 79, 367-379.

Goody, R. M., 1952: A Statistical Model for Water-Vapor Absorption. Q.J.R.M.S. 78, 165-169.

Goody, R. M., 1964: Atmospheric Radiation I: Theoretical Basis. Oxford University Press, 436 pp.

Goody, R. M., and M.J.S. Belton, 1967: Radiative relaxation times for Mars. Planet. Space Sci 15, 247-256.

Grandjean, J. and R. M. Goody, 1955: The concentration of carbon dioxide in the atmosphere of Mars; Astrophys, J., 121, 548-552.

Gray, L. D., 1965: Spectral emissivity calculations for the parallel bands of carbon dioxide at 4.3 microns. J.Q.R.S.T. 5, 569-583.

Hertzberg, G., 1945: Infrared and Raman spectra of polyatomic molecules. Van Nostrand, New York, 632 pp.

Hitschfeld, W., and J. T. Houghton, 1961: Radiative transfer in the lower stratosphere due to the 9.6 micron band of ozone. Q.J.R.M.S., 87, 562-577.

Hummer, D. G. and G. B. Rybicki, 1966: Non-LTE line formation with spatial variations in the Doppler width. Q.J.R.S.T. 6, 661-671.

Jones, L. M., and J. W. Peterson, 1967: Falling Sphere Measurements, 30 to 120 km. Univ. Michigan, Dept. Aerospace Engineering, Scientific Report 05627-12-S.

Kallmann-Bijl, H., R.L.F. Boyd, H. Lagow, S. M. Poloskov and W. Priester, 1961: Cospar international reference atmosphere, 1961. North-Holland Publishing Co, Amesterdam, 177 pp.

Kaplan, L. D., 1953: A quasi-statistical approach to the calculation of atmospheric transmission. Proc. Toronto. Meteor. Conf., 43-48.

Kaplan, L. D., 1959: A method for calculation of infrared flux for use in numerical models of atmospheric motion. The atmosphere and sea in motion, ed. B. Bolin. Oxford University Press, 509 pp.

Kaplan, L.D., 1967: Interpretation of the near infrared planetary spectra. Paper presented at Symposium on Molecular Structure and Spectroscopy, the Ohio State Univ., Columbus, Ohio Sept 5-9, 1967.

Kaplan, L. D., M. V. Migeotte and L. Neven, 1956: 9.6 micron band of telluric ozone and its rotational analysis. J. Chem Phys, 24, 1183-1186.

Kaplan, L. D., C. Münch and H. Spinrad, 1964: An analysis of the spectrum of Mars. Astrophys. J, 139, 1-15.

Kilore, A., D. L. Cain, G. S. Levy, V. R. Eshelman, G. Fjeldbo and F. D. Drake, 1965: Occulation experiment: results of the first direct measurements of Mars' atmosphere and ionosphere Science, 149, 1243-1248.

Kondrat'yev, K. Ya., 1965: Actinometry. Gidrometeorologicheskoye Izdalel'stvo, Leningrad. Translated by NASA (NASA TT-F-9712), 1965, 675 pp.

Kondrat'yev, K. Ya., I. Y. Badinov, G. N. Gaevskaya, G. A. Nikolsky and G. M. Shved, 1965: Radiative factors in the heat regime and dynamics of the upper atmospheric layers. Problems of atmospheric circulation, 47-75. Spartan Books, Washington D.C., 186 pp.

Kuhn, W. R., 1966: Infrared Radiative Transfer in the Upper Stratosphere and mesosphere. Scientific report, Dept. Astro-Geophysics, University of Colorado, 159 pp.

Ladenberg, R., and F. Reiche, 1913: Über selktive Absorption. Ann. Physik., 42, 181-184.

Leovy, C., 1964a: Radiative equilibrium of the mesosphere, J. atmos. Sci., 21, 238-248.

Leovy, C., 1964b: Simple models of thermally driven mesospheric circulation. J. Atmos. Sci., 21, 327-341.

Leovy, C. B. 1966: Radiative-convective equilibrium calculations for a two-layer Mars atmosphere. Rand Corporation Memorandum RM-5017-NASA, 42 pp.

Leovy, C. B. and Y. Mintz, 1966: A numerical general circulation experiment for the atmosphere of Mars. Rand Corporation Memorandum RM-5110-NASA, 42 pp.

Madden, R. P., 1961: A high resolution study of CO_2 absorption spectra between 15- and 18- microns. J. Chem. Phys., 35, 2083-2097.

Mayer, H., 1947: Los Alamos Scientific Lab. Report LA-647 (1947).

Mayot, M., and E. Vigroux, 1965: Application de l'approximation de Curtis-Godson a l'ozone atmospherique. Ann. de Geophys, 21, 80-105.

McCaa, D. J., and J. H. Shaw, 1967: Infrared absorption bands of ozone. Scientific Report No. AFCRL-67-0237, Ohio State University Research Foundation, 94 pp.

Minzner, R. A., K.S.W. Champion and H. L. Pond, 1959: The ARDC model atmosphere, 1959. Air Force surveys in geophysics, No. 115, 137 pp.

Mitchell, A.C.G., and M. W. Zermansky, 1934: Resonance Radiation and excited atoms, Cambridge Univ. Press, 338 pp.

Möller, F., 1963: On the influence of changes in the CO_2 concentration in air on the radiation balance of the earth's surface and on the climate. J. Geophy. Res., 68, 3877-3886.

Murgatroyd, R. J. and R. M. Goody, 1958: Sources and sinks of radiative energy from 30 to 90 km. Q.J.R.M.S., 87, 125-135.

Newell, R. E., 1967: Stratosphere and Mesosphere. Transactions of Am. Geophys. Union, 48, 436-449.

Ohring, G., and J. Marino, 1966: The vertical temperature distribution in the Martian atmosphere. J. Atmos. Sci 23, 251-255.

Penner, S. S., 1959: Quantitative molecular spectroscopy and gas emissivities. Addison-Wesley, Reading, Mass., 589 pp.

Peterson, J. W., 1967: Private communication.

Plass, G. N., 1956a: The influence of the 9.6 micron ozone band on the atmospheric infrared cooling rate. Q.J.R.M.S., 82, 30-44.

Plass, G. N., 1956b: The influence of the 15 micron carbon dioxide band on the atmospheric infrared cooling rate. Q.J R.M.S., 82, 310-324.

Prabhakara, C., and J. S. Hogan Jr., 1965: Ozone and carbon dioxide heating in the Martian atmosphere. J. Atmos. Sci. 22, 97-109.

Prabhakara, C., and J. S. Hogan, Jr., 1966: Equilibrium temperature structure in the mesophere and lower-thermosphere. New York Univ., Geophys. Sci, Lab. Report No. TR-66-1, 35 pp.

Ray, G. W., W. E. Deeds and A. H. Nielsen, 1966: An Investigation of the Effect of Multiple Absorption and Emission of Resonance-Line Photons on Line Shape and Line intensity. University of Tennessee, Dept. of Physics, Technical Report.

Read, A. W., 1965: Vibrational relaxation in gasses. Progress in Reaction Kinetics, 3, 203-235.

Rodgers, C. D., and C. D. Walshaw, 1966. The computation of infrared cooling rate in planetary atmospheres. Quart. J. Roy. Meteor. Soc., 92, 67-92.

Sasamori, T., and J. London, 1966: The decay of small temperature preturbations by thermal radiation in the atmosphere. J. Atmos. Sci 23, 543-554.

Shved, G. M., 1964: Approximation of the single line during the transfer of radiant energy in the upper atmosphere. Bull. Leningrad State Univ. No. 4, Physical and Chemical Series. Translated as Rand report. (P-3595).

Shved, G. M., 1965a: Method of allowing for the deviation from Kirchoff's law in the mesosphere for radiative transfer in the 15 μ CO_2 band. Bull. Leningrad State Univ No. 4, Physical and Chemical Series. (Translated as Rand report P-3597).

Shved, G. M., 1965b: On the heating effect of the 15 micron band of carbon dioxide in the upper atmosphere. Problems on Physics of the atmosphere. Problems on Physics of the atmosphere, Leningrad State Univ. (Translated as Rand report P-3596).

Stull, V. R., P. J. Wyatt and G. N. Plass, 1963: The Infrared Absorption of Carbon Dioxide, Infrared transmission studies, Final Report, SSD-TDR-62-127 Vol III, Aeronutronics Division, Ford Motor Co.

Theon, J. S., W. Nordberg, L. B. Katchen and J. J. Hovarth, 1967: Some observations on the thermal behavior of the mesosphere. J. Atmos. Sci. 24, 428-438.

U.S. Standard Atmosphere, 1962: U.S. Government printing office, Washington D.C., 278 pp.

Walshaw, C. D., 1957: Integrated absorption by the 9.6 μ band of ozone. Quart. J. Roy. Meteor. Soc, 83, 315-321.

Walshaw, C. D., and C. D. Rodgers, 1963: The effect of the Curtis- Godson approximation on the accuracy of radiative heating-rate calculations. Q.J.R.M.S., 89, 122-130.

Winters, B. H., S. Silverman and W. S. Benedict, 1964: Line Shape in the Wing Beyond the Band Head of the 4.3 μ band of CO_2. J.Q.S.R.T., 4, 527-537.

Wyatt, P. J., V. R. Stull and G. N. Plass, 1962. Quasi Random Model of Band Absorption. J. Opt. Soc. Am., 52, 1209-1217.

Young, C., 1964: A Study of the influence of Carbon Dioxide on Infrared Radiative Transfer in the Stratosphere and Mesosphere. Tech. Report, Dept of Meteorology and Oceanography, Univ. Michigan, 176 pp.

Young, C., 1965: Calculation of the absorption coefficient for lines with combined Doppler and Lorentz broadening. J. Quant. Spect. Rad. Trans. 5, 549-552.